THE RELATIONSHIP BETWEEN THE DEPTH TO THE 0°C ISOTHERM OF THE ARCTIC OCEAN AND ATMOSPHERIC FORCING

By

Moon, Sookmi

RECOMMENDED:

Uma K Bhatt

Mark A Johnson

Advisory Committee Chair

Head, Program in Marine Sciences and Limnology

APPROVED:

Dean, School of Fisheries and Ocean Sciences

Susan McHenrichs

Dean of the Graduate School

April 12, 2004

Date

THE RELATIONSHIP BETWEEN THE DEPTH TO THE 0°C ISOTHERM OF THE ARCTIC OCEAN AND ATMOSPHERIC FORCING

A

THESIS

Presented by the Faculty

of the University of Alaska Fairbanks

in Partial Fulfillment of the Requirements

for the Degree of

MASTER OF SCIENCE

By

Sookmi Moon, M.S.

Fairbanks, Alaska

May 2004

Abstract

Empirical Orthogonal Function (EOF) analyses of the depth to the 0°C isotherm of the Arctic Ocean were performed to determine the variability of the depth to the 0°C isotherm in the Arctic Ocean. The data are from the "Environmental Working Group – Joint U.S. Russian Atlas of the Arctic Ocean". The first three modes explain 99% of the total variance with each mode explaining 51%, 26%, and 23%, respectively. Mode 1 shows the pattern of the outflow through Fram Strait and the Lincoln Sea. Mode 2 shows the variability of the inflow from the Barents Sea and the variability of the outflow through the Canadian Archipelago as well as the variability of the Transpolar Drift. Mode 2 has a close relationship with atmospheric conditions (Arctic Oscillation or North Atlantic Oscillation index). Mode 3 is significantly correlated with the annual mean vorticity index, when the vorticity index leads by 1 year. Composite analyses of the data using the AO, NAO, and vorticity index confirm that the EOF analyses of this study are valid. This study shows that the variability of the 0°C isotherm of the Arctic Ocean is significantly correlated with atmospheric conditions.

Table of Contents

List of Figures

List of Tables

Acknowledgements

I would like to thank my advisor, Mark Johnson. He accepted me into the program and introduced me to the ways of the Arctic Ocean, which is a very interesting place to study. I feel very lucky having him as my advisor. I would also like to thank my thesis committee members, Uma Bhatt, Tom Weingartner, and Igor Polyakov for their advice on this work.

For my study, Matlab was a main tool that I worked with, but I didn't even know 'm' of Matlab (Korean expression). Many friends helped me whenever I struggled with Matlab: Seth, Hank, Bill, Jeremy, and Sarah. Thank you, guys. I had to face disk failure just when I was ready to start to write. All the work I did was gone. It was quite a nerve-wracking experience. I hope I said enough thanks to the IT guys, sweet Steve, Rob, and Mark. I shouldn't forget to thank Rachel, who read through my thesis with a strong English background (her mom is an English teacher).

I would like to say 'thank you' to all my friends for their mental support. Lastly, I would like to give special thanks to my husband Joel Young (of course) for his great support. He always made sure that I didn't work too hard and took enough rest. I also thank my family for their support.

This research was funded by the NSF/IARC Arctic Ocean Model Intercomparison Project (AOMIP) and a UAF Thesis Completion Fellowship

Chapter 1. Introduction

The Arctic region is expected to be one of the most sensitive areas to global climate change. Despite its importance for the global climate, it has not been easy to collect observations due to limited accessibility. Recent research reveals signs of warming in the Arctic Ocean, such as a decrease in ice cover, a strengthened Atlantic inflow, and warmer temperature of the Atlantic layer [Swift et al., 1997; Zhang et al, 1998; Grotefendt et al., 1998; Dickson et al., 2000]. These changes of the Arctic are related to atmospheric conditions, mostly represented as North Atlantic Oscillation (NAO) or Arctic Oscillation (AO) indices [Loeng et al., 1997; Zhang et al., 1998; Blindheim et al., 2000; Morison et al., 2000].

Warming in the Arctic Ocean is shown by warmer temperatures of the Atlantic layer possibly induced by the Atlantic inflow to the Arctic Ocean. Since the Atlantic Water is identified as the water warmer than 0°C in the Arctic Ocean, it is logical to examine the 0°C isotherm. One way to examine such data is through Empirical Orthogonal Function (EOF) analysis, which is also known as Principal Component analysis. An EOF analysis of the 0°C isotherm will show how the interface between the surface water and the Atlantic Water responds in time. The only dataset that has long enough records with sufficient geographical cover to do an EOF analysis is from the Atlas of the Arctic Ocean by the Environmental Working Group (EWG), which is compiled from Russian Climatoligies and United States buoy observations.

Grotefendt et al. (1998) argued that a limited number of discrete data from bottles (the Russian data are discrete data) lead to errors in determining the temperature maximum of the water column. However, interpolating the 0°C isotherm depth should have significantly less errors than deciding the temperature maximum of the water column from bottle data. This is because the 0°C point is interpolated from a linear line, while the temperature maximum needs to be interpolated from a nonlinear curvature.

The goal of this study is to determine whether the depth to the 0°C isotherm of the Arctic Ocean contains recognizable patterns of decadal or longer variability. The specific steps are as follows:

1) to perform an EOF analysis on the depth to the 0°C isotherm of the Arctic Ocean and to find out how the 0°C isotherm changes in time and what the EOF patterns show,
2) to compare the EOF time series with the Arctic Oscillation (AO) index, the North Atlantic Oscillation (NAO) index, and the annual mean vorticity index of the Arctic Ocean, and to look for relationships between 0°C isotherm depths and atmospheric conditions, and
3) to perform composite analyses of the depth to the 0°C isotherm based on atmospheric indices and to validate the EOF analysis performed in this study.

Chapter 2. Literature Review

2.1 Introduction to the Arctic Ocean

The Arctic Ocean is called the Arctic Mediterranean Sea along with the Greenland/Iceland/Norwegian (GIN) sea system [Carmack,1990; Rudels and Friedrich, 2000]. This means that the Arctic Ocean has limited communication with the major oceans, and its circulation is dominated by thermohaline forcing. The Arctic Ocean is connected to the Pacific Ocean through Bering Strait and connected to the Atlantic Ocean through Fram Strait, the Barents Sea, and the Canadian Archipelago. Because the dynamic height of the Pacific is higher than the Atlantic, Bering Strait water mostly flows into the Arctic Ocean. The outflow of the Arctic Ocean is mainly through the Canadian Archipelago and Fram Strait. The Atlantic Water comes into the Arctic Ocean through Fram Strait and the Barents Sea. Although it has been known that most of the Atlantic inflow to the Arctic Ocean is west of Svalbard through Fram Strait as the West Spitsbergen Current, recent observations reveal that the Atlantic inflow through the Barents Sea may be as great as, or perhaps greater than, the inflow through Fram Strait [Rudels et al., 1994].

2.1.1 Water Masses of the Arctic Ocean

The Arctic Ocean is a strongly stratified ocean mainly composed of three layers: a surface layer, an intermediate layer, and the deep water. The density of the surface

layer is less than σ_0=27.9; the intermediate layer is greater than σ_1=32.785; and the deep water is less than σ_2=37.457 [Aagaard et al., 1985].

The surface water in the Arctic is called Polar Water. It is the water of admixture with fresher shelf waters and has temperatures between 0°C to freezing temperature (-1.5 to –1.9°C) and salinities below 34.4. The lower part of the surface layer includes the cold halocline, one of the main features of the Arctic Ocean. This cold halocline has salinities between 30.4 and 34.4 and temperatures less than -1°C.

The intermediate layer is mainly from the Atlantic Water. The Atlantic Water enters into the Arctic Mediterranean Sea as a branch of the Norwegian-Atlantic Current with temperatures above 3°C and salinities higher than 34.9. As the Atlantic Water flows northward and mixes with other water masses, its temperature and salinity starts to decrease. The Atlantic layer in the Arctic Ocean has the same salinity as the deep water but much warmer temperatures. When the Atlantic Water enters the Arctic Ocean, it is covered by the cold halocline, which is strongly stable and will not easily mix with other waters. Therefore, the properties of the Atlantic layer change relatively little in the Arctic Ocean. The core of the Arctic Intermediate Water, including the Atlantic layer, is identifiable over the entire basin at depths between 200m to 800m. The layer includes the temperature maximum of the water column [Carmack, 1990].

Deep waters, if defined as lying below the lower 0°C isotherm, constitute about 60% of the water in the Arctic Ocean [Aagaard, 1981]. Four water masses have been recognized. Canadian Basin Deep Water is the most saline (>34.95) and warmest

(about –0.5°C), and Greenland Sea Deep Water is the freshest (<34.9) and coldest (about –1.2°C). In between are Eurasian Basin Deep Water (34.94,-0.7°C) and Norwegian Sea Deep Water (34.92,-0.9°C) [Carmack, 1990].

2.1.2 Currents and Circulation

Two main currents flow through Fram Strait, exchanging water with the Atlantic Ocean. The East Greenland Current, following the east coast of Greenland, is the main outflow of the Arctic Ocean. The East Greenland Current carries sea ice, surface water, intermediate water, and deep water from the Arctic equatorward. The West Spitsbergen Current is the extension of the Norwegian Atlantic Current, flowing along the west coast of Svarbard. The West Spitsbergen Current carries Atlantic Water, Arctic Intermediate Water, and Greenland and Norwegian Deep Waters poleward. Having a sill depth of 2500m, Fram Strait allows water to flow at deep depths [Aagaard et al, 1987, Carmack 1990].

The main features of the Arctic Ocean's surface circulation are the Transpolar Drift and the Beaufort Gyre. The Transpolar Drift carries sea ice and surface water from the Siberian shelves to Fram Strait, exiting as part of the East Greenland Current. The Beaufort Gyre is an anticyclonic gyre in the Canada Basin. The circulation of the Atlantic layer and intermediate depth waters is composed of several cyclonic loops [Rudels et al, 1994; Jones, 2001]. Figure 2.1 shows the schematic circulations of surface water and the Atlantic layer. The Barents Sea branch water meets the Fram Strait branch water after exiting the St. Anna Trough

and follows the Eurasian Basin Slope. When this flow meets the Lomonosov Ridge, one part makes it over the ridge, and the other part turns to follow the ridge forming a loop in the Eurasian Basin [Rudels and Friedrich, 2000]. Only a fraction of the inflow, primarily the Barents Sea branch with a smaller portion of the Fram Strait branch, crosses over the Lomonosov Ridge [Rudels et al., 1994].

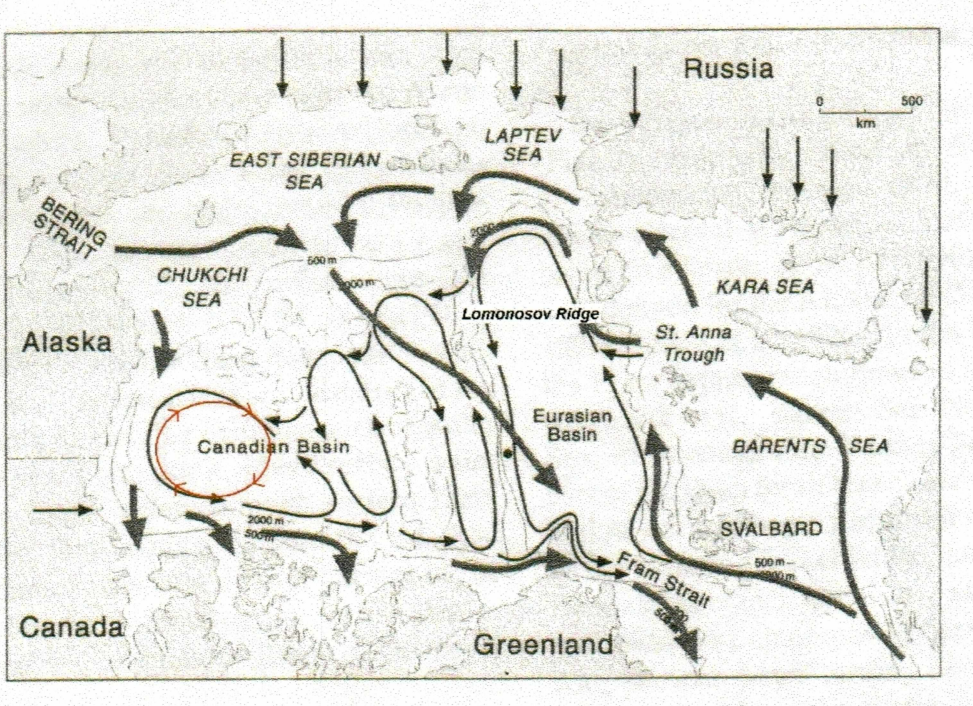

Figure 2.1 Schematic circulation of surface water (grey thick line) and the Atlantic layer (black thin line). Red circle shows the anticyclonic Beaufort Gyre. Modified from E.P. Jones (2001).

2.2 Atlantic Water in the Arctic Ocean

When the Atlantic water enters the Arctic Mediterranean as the Norwegian Atlantic Current, it starts to rapidly decrease its initial high temperature and salinity by losing heat to the atmosphere and by mixing with local waters. As this current flows northward, it divides into two branches at the latitude of the Barents Sea. One part becomes the West Spitsbergen Current, passing through Fram Strait, and the other enters the Barents Sea. Some of the West Spitsbergen Current turns west and flows back underneath the Polar Water of the East Greenland Current, which is the main outflow of the Arctic Ocean. This returning West Spitsbergen Current is often called the Return Atlantic Current [Bourke et al., 1988]. The rest of the West Spitsbergen Current enters the Arctic Ocean. The West Spitsbergen Current encounters an ice margin northwest of Spitsbergen and is further cooled and diluted by melting ice. From here, Atlantic Water is identified by temperatures above 0°C in the Arctic Ocean at depths between 100-800m. Nansen first observed the warm temperature ($\theta > 0°C$) associated with the Atlantic layer during the Fram Expedition [Rudels et al., 1994]. The Atlantic layer can be followed by the 0°C isotherm throughout the Arctic Ocean mostly due to the existence of the cold halocline. The cold halocline is the layer in which salinity changes abruptly. Therefore, this layer is strongly stable and does not allow neighboring upper and lower layers to mix with each other. Since the cold halocline acts as a stable cover, the Atlantic layer does not mix with the surface layer, nor melt the sea ice.

In the Barents Sea, Atlantic Water experiences intense heat loss at the sea surface and mixing with fresh water from melting ice, river runoff, and the Norwegian Coastal Current. It is also subjected to salt injection due to brine rejection from freezing ice. As a result, a variety of water is formed in the Barents Sea. The Barents Sea branch Atlantic Water is the densest water on the eastern part of the Barents Sea Shelf [Karcher and Oberhuber, 2002]. By the time the Barents Sea branch Atlantic Water flows into the Arctic Ocean, this branch is colder and fresher and dominates at greater densities, while Fram Strait branch is warmer and more saline and dominates at lesser densities [Rudels et al., 1994, Rudels and Friedrich, 2000].

The estimates of the Atlantic inflow into the Arctic Ocean have varied with different observations for the last 30 years. Aagaard and Greisman (1975) proposed an inflow of 7.1 Sv Atlantic Water in the West Spitsbergen Current and an outflow of 1.8 Sv Polar Water and 5.3 Sv modified Atlantic Water in the East Greenland Current. However, later work found that the West Spitsbergen Current bifurcates into a westward turning branch and an eastward or inshore branch. The westward turning branch follows the Yermak Plateau and joins the recirculation of Atlantic Water in Fram Strait [Aagaard et al., 1987; Bourke et al., 1988], which results in smaller estimates of the Atlantic inflow actually entering the Arctic Ocean. The recent observations show that the amount of Atlantic inflow through the Barents Sea may be similar to or greater than that through Fram Strait at different times [Rudels, 1987].

2.3 Climate Indices

2.3.1 North Atlantic Oscillation Index

The atmospheric system of the North Atlantic may be characterized by the difference between the Icelandic low pressure cell and the Azores (or Portugal, Gibraltar) high pressure cell. The North Atlantic Oscillation (NAO) is a seesaw pattern of these two pressure cells. When the pressure over Iceland is lower than normal, the Azores high pressure is higher, and vice versa. The NAO index is defined as the difference of sea-level pressure between the Icelandic low and the Azores high. In calculating the indices, several locations have been used for the southern station, while the northern station has consistently been Stykkisholmur, Iceland. In this study, the winter index (December through March) of Hurrell (1995) is used, which is the difference between normalized pressures at Stykkisholmur, Iceland, and Lisbon, Portugal.

The NAO can affect the Atlantic layer of the Arctic Ocean in two ways. First, since the Norwegian Atlantic Current originates from the North Atlantic, the temperature of the Atlantic inflow depends on the weather of the North Atlantic region. Second, the volume transport of Atlantic Water through Fram Strait and the Barents Sea is related to the atmospheric pressure (When the Icelandic low is stronger than normal, more Atlantic Water makes it through Fram Strait and Barents Sea Opening) [Loeng et al., 1997; Zhang et al., 1998].

2.3.2 Arctic Oscillation Index

The Arctic Oscillation (AO) Index comes from the leading EOF of monthly (or winter time mean) sea-level pressure anomalies over the region poleward of 20°N [Thomson and Wallace, 1998]. The EOF shows an oscillating pattern of atmosphere between the polar region and the region of mid latitudes (37-45N). The positive phase is induced from lower than normal pressure over the polar region and higher than normal pressure in the mid latitudes. This larger difference of pressures between two areas enhances Westerlies in the north Atlantic and warmer and wetter weather in northern Europe.

According to Deser (2000), the teleconnectivity between the Arctic and the mid latitudes is strongest over the Atlantic sector, and the temporal coherence between the Atlantic and Pacific mid latitudes is weak. Hence, the AO time series is nearly indistinguishable from the leading structure of variability in the Atlantic sector.

2.4 Atmospheric Condition and Atlantic Water

The strength of the Atlantic inflow is related to the prevailing atmospheric conditions, especially for the Barents Sea. It is shown that the highest inflow of Atlantic Water occurs during low pressure years in the Barents Sea, while there is reduced flow in years with high pressure [Ådlandsvik and Loeng, 1991; Loeng et al., 1997]. In the late 1980s and 1990s, there was a substantial decrease in sea level pressure, characterized by a strengthening of the Icelandic low and a weakening of

the Beaufort high. During this time, a strengthened Atlantic inflow was observed [Walsh et al., 1996; Morison et al., 1998].

Proshutinsky and Johnson (1997) proposed that there are two regimes of wind-driven motion in the central Arctic, alternating between anticyclonic and cyclonic circulation. They argued that the upper layer moves toward the center in the anticyclonic circulation due to Ekman transport, raising sea level in the middle and lowering it along the coasts. During the cyclonic regime, the opposite takes place (Figure 2.2).

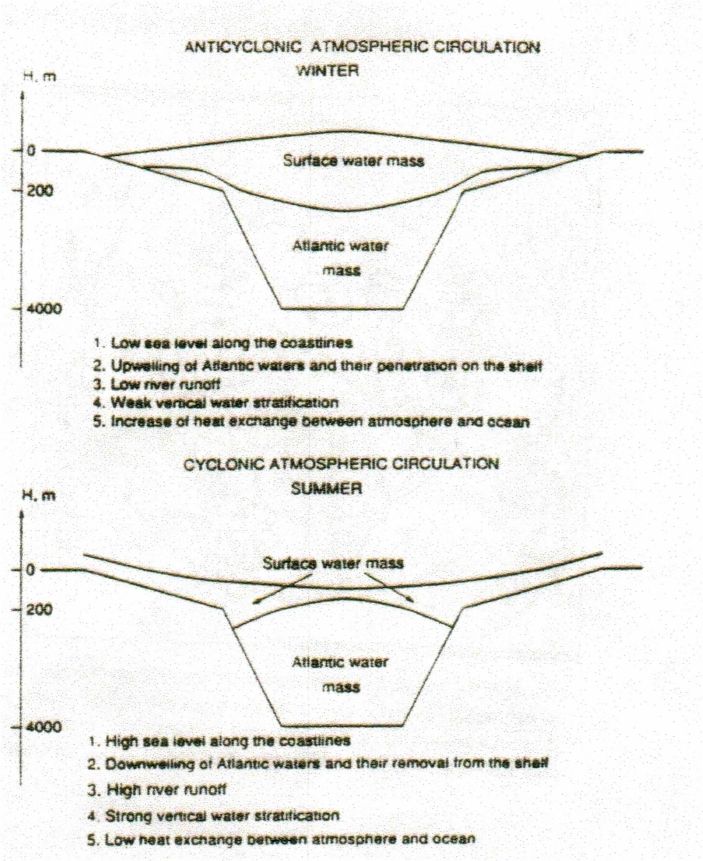

Figure 2.2 Schematic water mass structure and prevailing processes. Proshutinsky and Johnson (1997).

In Figure 2.2, the boundary between the Surface water and the Atlantic Water can be identified as the 0°C isotherm. Proshutinsky and Johnson showed that the depth to the 0°C isotherm might vary with different atmospheric conditions. If the 0°C isotherm undulates with variable conditions, an EOF analysis of the depth to the 0°C isotherm will allow us to find patterns of oscillation in time and space. With the pattern found, it can be related to atmospheric indices. This study seeks to disprove the hypothesis that the variability of the depth to the zero degree isotherm of the Arctic Ocean shows no relationship to atmospheric variability.

Chapter 3. Data and Methods

3.1 Data

The depth to the 0°C isotherm data that are used for the EOF analysis, are from the CD-ROM titled "Environmental Working Group (EWG) - Joint U.S. Russian Atlas of the Arctic Ocean". The EWG was formed to find ways of combining the separate scientific strengths and data resources on the Arctic Ocean of both countries. This atlas is based upon more than one million observations collected over the period 1948-1993 from Russian drifting stations, ice breakers, and airborne expeditions. U.S. buoy observations were also used in the atlas. The data can be obtained through www.nnic.noaa.gov/atlas/ or by purchasing a CD-ROM. There are two different datasets: one for winter and one for summer. The winter period dataset was used in this study.

The temporal distribution of EWG data is shown in Figure 3.1. For the time span of 1950 – 1989, which is the period of the data used for this study, there are less data in the early 50's and early 80's so that the number of data in the middle 80's and late 80's increased significantly compared to the earlier period.

The locations of western (European and North American countries) and Russian hydrographic stations are shown in Figure 3.2 and Figure 3.3. Overall, the Russian stations are evenly distributed over the whole Arctic between 1950's and 1970's. Western stations are found mostly in the GIN Sea.

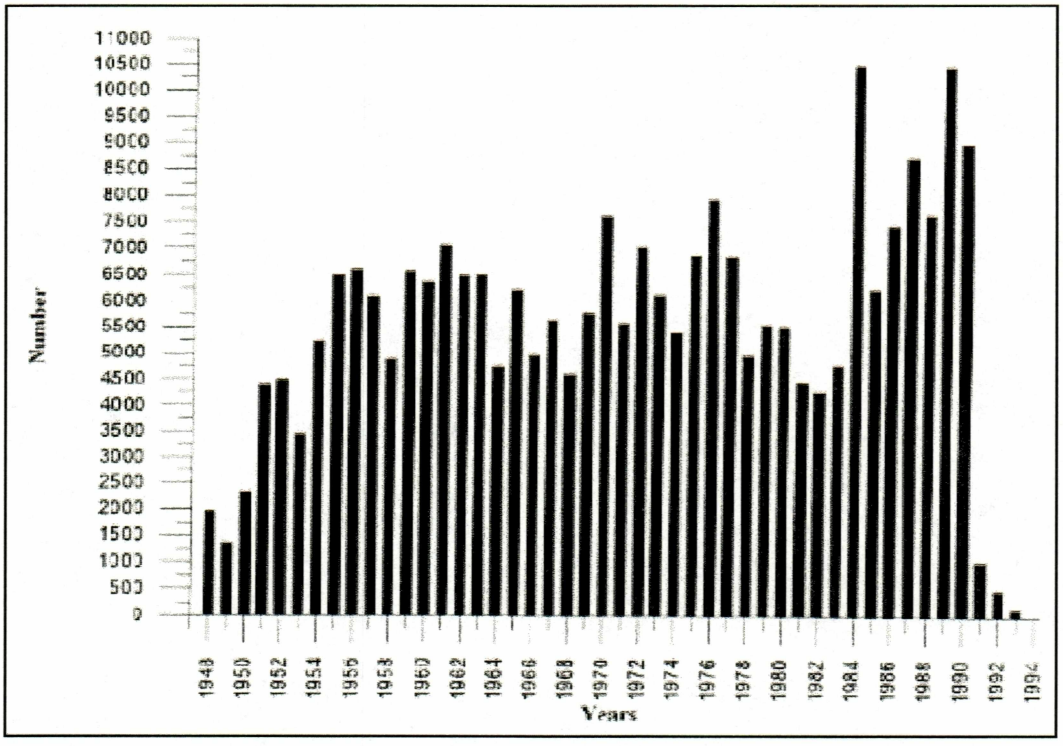

Figure 3.1 Temporal distribution of EWG data.
(Environmental Working Group, Oceanography Atlas for the Winter Period, 1997)

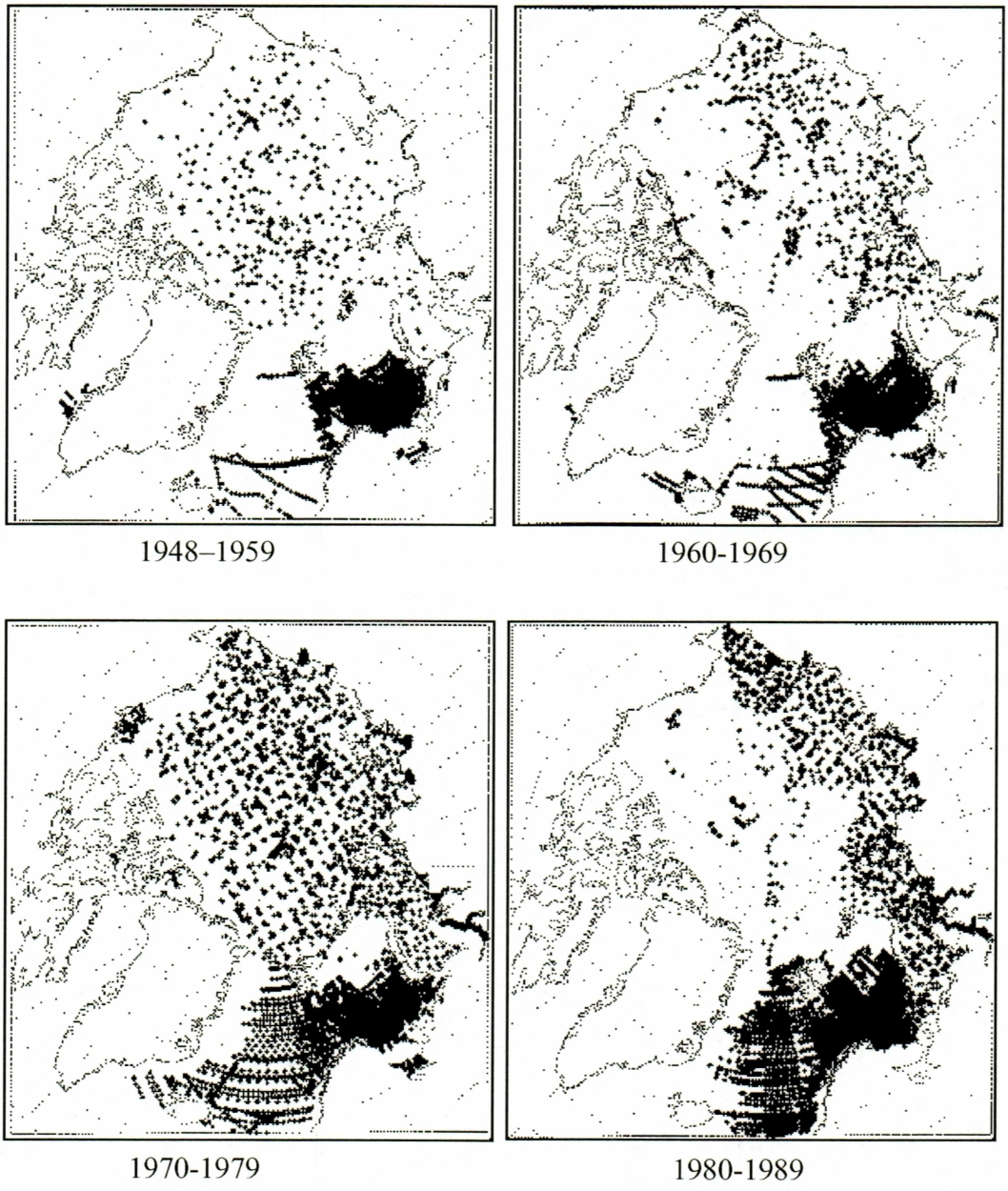

Figure 3.2 Russian stations, 1948-1989.
(Environmental Working Group, Oceanography Atlas for the Winter Period, 1997)

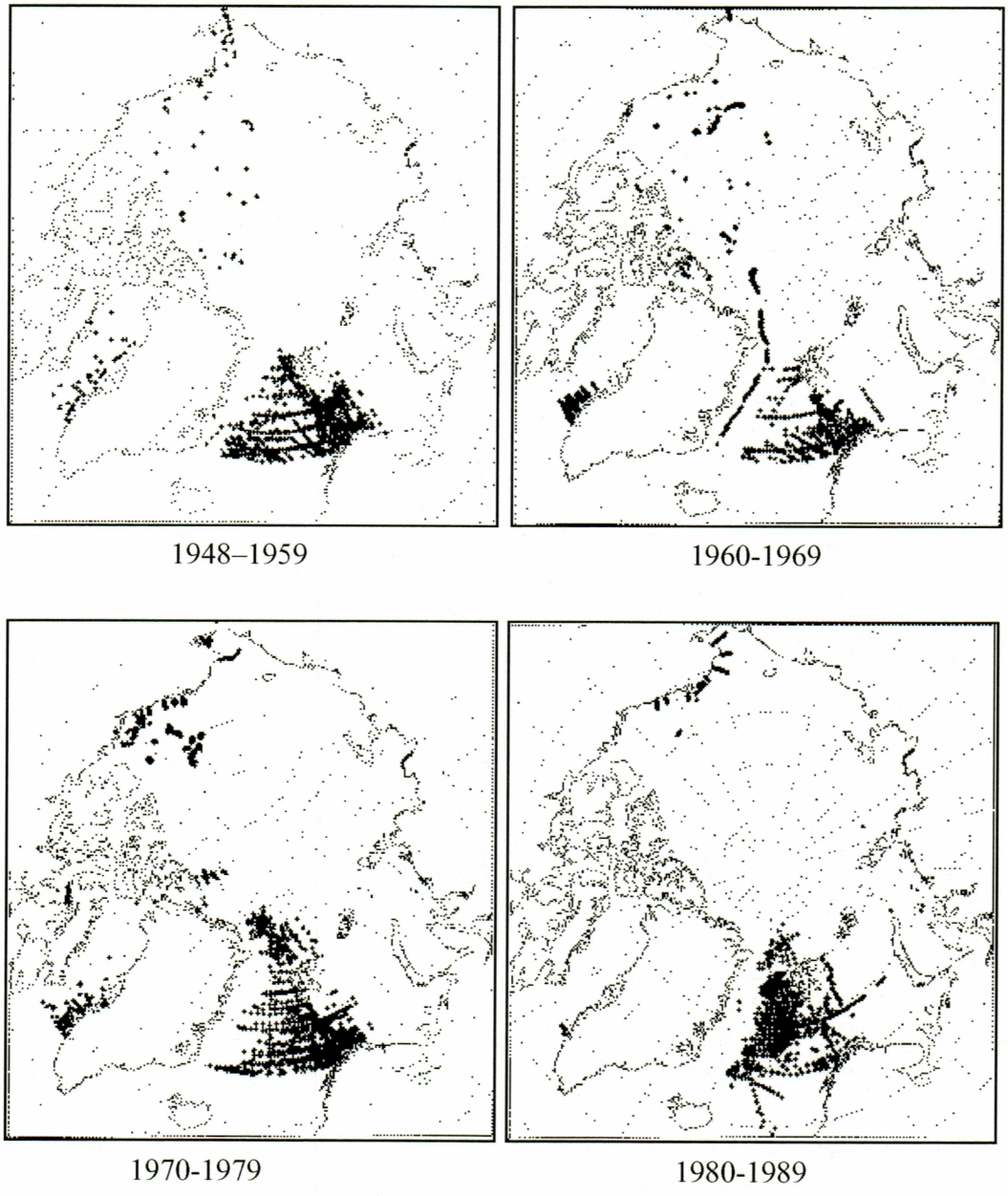

Figure 3.3 Western stations, 1948-1989.
(Environmental Working Group, Oceanography Atlas for the Winter Period, 1997)

Data sparse areas needed special averaging and interpolation techniques to obtain acceptable results. Four separate methodologies were used to derive gridded mean fields. The resulting individual fields were consistent with one another. The method of spectral objective analysis was chosen to make the grids, which are mapped in the climatic atlas.

The depths to the zero degree isotherm are found from the temperature profiles of all locations and are given by EWG. The data points from the central Arctic basin are shown in Figure 3.4. The grid cell size is approximately 171×171 km and there are 169 grid points for the central Arctic. The data used are from winter months, December through May, from 1950 to 1989. The years of missing data are 1951, 1952, 1953, 1964, 1969, 1986, and 1987. Therefore, 33 years are available in the time span.

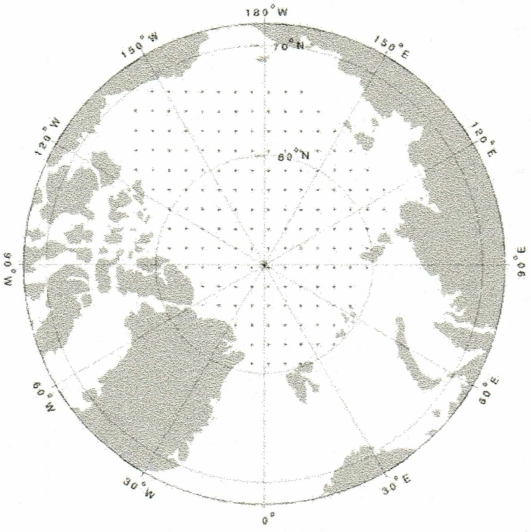

Figure 3.4 Data points of the study area

3.2 Empirical Orthogonal Function (EOF) Analysis

Empirical Orthogonal Function (EOF) analysis is a statistical analysis commonly known as Principal Component analysis. In oceanography and meteorology, it is often necessary to analyze a large set of spatial and temporal data. EOF analysis provides a compact description of a large dataset in terms of orthogonal functions. EOFs can be derived as below, following Emery and Thomson (2001).

If there are M locations and N different measurements at all locations, the data series $\psi_m(t)$ can be written as

$$\psi(x_m,t) = \psi_m(t) = \sum_{i=1}^{M}[a_i(t)\phi_{im}] \tag{3.1}$$

where x_m is any given location, $\phi_i(x_m) = \phi_{im}$ are the orthogonal spatial functions, and $a_i(t)$ is the amplitude of the ith orthogonal mode at time t. The time series of the dependent scalar variable $\psi_m(t)$ at each location x_m is the linear combination of M spatial functions, ϕ_i. The spatial functions are weighted by time-dependent coefficients, $a_i(t)$. Here, all $\phi_i(x_m)$ need to be orthogonal to each other:

$$\sum_{m=1}^{M}[\phi_{im}\phi_{jm}] = \delta_{ij} \tag{3.2}$$

Equation (3.2) is an orthogonality condition, and δ_{ij} is the Kronecker delta:

$$\delta_{ij} = 1, \text{ if } j = i$$

$$= 0, \text{ if } j \neq i$$

To get unique EOFs, the time amplitudes need to be uncorrelated over the sample data. This means that the time averaged covariance of the amplitude satisfies

$$\overline{a_i(t)a_j(t)} = \lambda_i \delta_{ij} \tag{3.3}$$

The overbar denotes the time-averaged value. Equation (3.3) can be changed as below.

$$\lambda_i = \overline{a_i(t)^2} = \frac{1}{N}\sum_{n=1}^{N}[a_i(t_n)^2] \tag{3.4}$$

where λ_i is the variance of each orthogonal mode. If we then compute the mean product matrix $\overline{\psi_m(t)\psi_k(t)}$ with the known data, and use equation (3.3), then

$$\begin{aligned}\overline{\psi_m(t)\psi_k(t)} &= \sum_{i=1}^{M}\sum_{j=1}^{M}[a_i(t)a_j(t)\phi_{im}\phi_{jk}] \\ &= \sum_{i=1}^{M}[\lambda_i\phi_{im}\phi_{jk}]\end{aligned} \tag{3.5}$$

Multiplying both sides of the equation (3.5) by ϕ_{ik}, summing over all k, and using the orthogonality condition (3.2) yields

$$\sum_{k=1}^{M}\overline{\psi_m(t)\psi_k(t)}\phi_{ik} = \lambda_i\phi_{im} \quad (i\text{th mode at } m\text{th location; } i,m = 1,\ldots,M) \tag{3.6}$$

Here, the EOFs, ϕ_{im}, are the ith eigenvectors at locations x_m and λ_i are the corresponding eigenvalues. If the mean value of the time series $\psi_m(t)$ is removed at each site x_m, equation (3.6) can be written in matrix notation:

$$C\phi - \lambda I\phi = 0 \tag{3.7}$$

where C is the covariance matrix, which consists of M data series of length N with elements. I is the unity matrix.

The variance of the first mode, λ_1 has the greatest percentage of the total variance. Of the remaining variance, the greatest is the second mode, λ_2, and so on. Hence, the total variance of all the time series is

$$\sum_{m=1}^{M} \frac{1}{N} \sum_{n=1}^{N} [\psi_m(t_n)]^2 = \sum_{j=1}^{M} \lambda_j \tag{3.8}$$

The sum of the variances in the data equals the sum of the variance in the eigenvalues. Lastly, the time-dependent amplitudes of the *i*th statistical mode can be determined as follows:

$$a_i(t) = \sum_{m=1}^{M} \psi_m(t) \phi_{im} \tag{3.9}$$

Using equation (3.6), the EOFs can be found. After computing the mean product matrix, $\overline{\psi_m(t)\psi_k(t)}$ (m,k =1,…,M), the eigenvectors and eigenvalues can be determined using standard computer algorithms. The variance of each mode, λ_i, and the time-dependent amplitudes, $a_i(t)$ is then obtained.

Often, the first few EOFs with large variances can be used to describe the fundamental variability in a large data set. It may be useful to employ the EOFs to eliminate unwanted small variability. So, using a limited number of EOFs, the data field can be reconstructed, and an EOF analysis is then performed to obtain a new apportionment of the variance. Conventional EOF analysis can be used to find standing oscillation only. There are other kinds of EOF analysis, using, for example, a lagged covariance matrix, or complex principal component analysis.

3.3 Application of EOF for This Study

Since there are 169 points in the study area and 33 years of time period, the size of the data matrix formed is 33×169. The time mean of each point is then subtracted from the data to obtain the anomalies. With the anomalies of the data, the symmetric covariance matrix (169×169) is formed, which is then decomposed into eigenvectors and eigenvalues. Successively, the time series of the amplitudes for each mode are calculated. Eigenvectors are so called EOFs, which show a pattern of each mode. Eigenvalues explain the variance of each mode. A variance is calculated by dividing an eigenvalue by the total of eigenvalues.

Chapter 4. Results and Discussion

4.1 Statistics of the Data

The depth to the 0°C isotherm in the study area ranges between 50m and 350m. The mean depth of each point is shown in Figure 4.1.a. As the Atlantic Water enters into the Arctic Ocean at Fram Strait, the 0°C depth is found around 100 m. The depth becomes deeper as the water flows counterclockwise around the Arctic basin. In the Eurasian Basin, the depths are between 100m and 200m. The return flow of the Atlantic layer in the Eurasian Basin has a depth range around 200m. After the Atlantic Water passes over the Lomonosov Ridge, the 0°C depth gets deeper than 200m in the Makarov Basin. Finally, in the Canada basin, the depths are the deepest, ranging around 300m, and the deep isotherm clearly shows the Beaufort Gyre.

The variability of the depths over time is the highest in Fram Strait, where its standard deviation is greater than 20. The second highest variability is the area where the Pacific water flows in from Bering Strait (the upper left corner of the study area in Figure 4.1.b). This suggests the area where foreign water flows in has more variability. The area neighboring the Siberian Sea has high variability as well. The Canada Basin with dark blue and white colors has the lowest variability. Overall, the variability of the Eurasian Basin is higher than that of the Canadian Basin.

a)

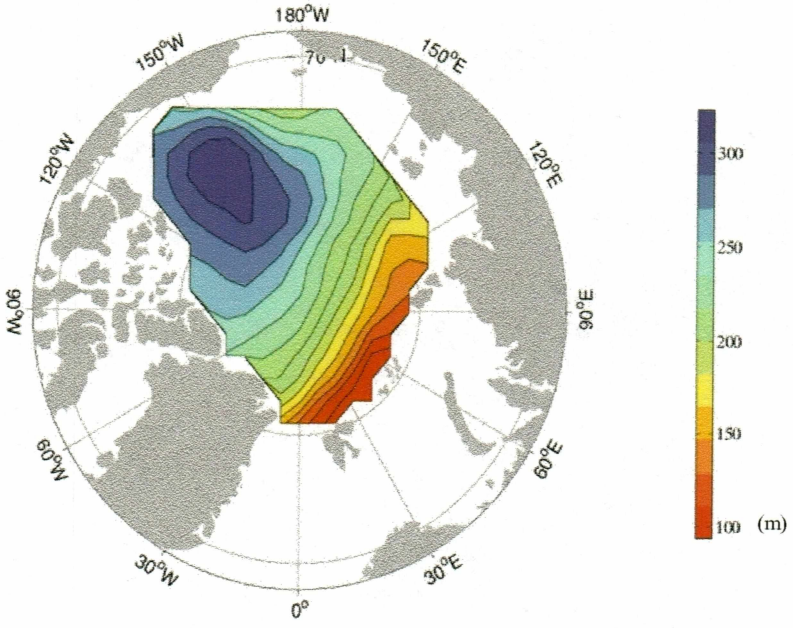

b)

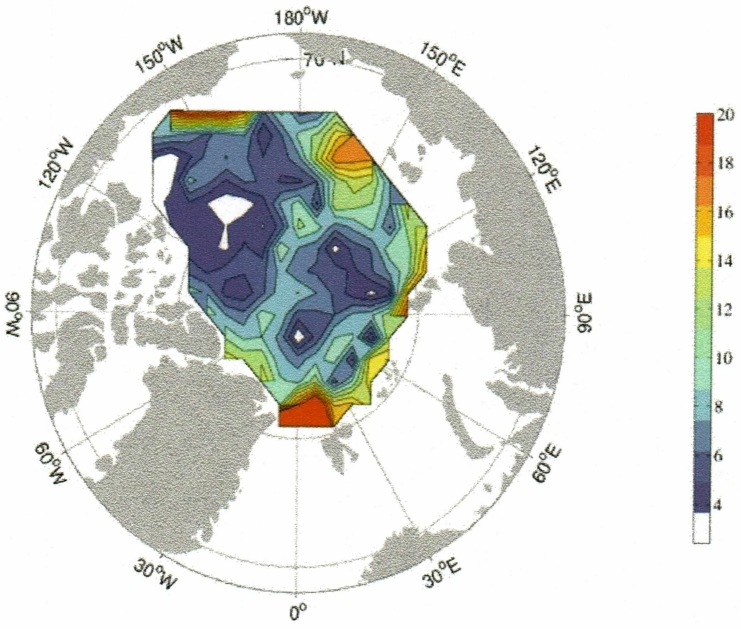

Figure 4.1 a) Mean depth and b) standard deviation of depth to the 0°C isotherm.

4.2 EOF Analysis

4.2.1 The EOF Analysis (Central Arctic)

The first three EOFs of the Central Arctic are shown in Figure 4.2. The variances of these modes are 50.64%, 26.01%, and 23.34%, respectively. The first three modes show more than 99% of the variability, and the other modes are noise. Mode 1 shows that the largest anomaly is in Fram Strait. The area north of Greenland, including the Lincoln Sea has a high anomaly, as well. This high variability in the vicinity of Fram Strait probably has to do with the large amount of water being exchanged through Fram Strait (East Greenland Current, 11.1± 1.7 Sv; West Spitsbergen Current, 9.5 ± 1.4 Sv) [Fahrbach et al, 2001].

Mode 2 shows higher amplitude in the area where the Barents Sea water flows out, following the Eurasian Basin Slope and the area neighboring the Laptev and Siberian Shelves. These areas have reddish colors, which means that the depths to the 0°C isotherm are deeper than the average, when the time series is positive. The rest of the area is generally negative in sign, meaning shallower 0°C depths than the average. The blue area, starting near the Chukchi Sea and crossing the Arctic Ocean resembles the path of the Transpolar Drift. The other blue line follows the path of Pacific-origin waters, which exit mainly through the Canadian Archipelago [McLaughlin et al., 2002]. Therefore, mode 2 suggests that changes in inflow from the Barents Sea and changes in outflow of Arctic water through the Canadian Archipelago as well as changes in the Transpolar Drift happen at the same time.

Mode1

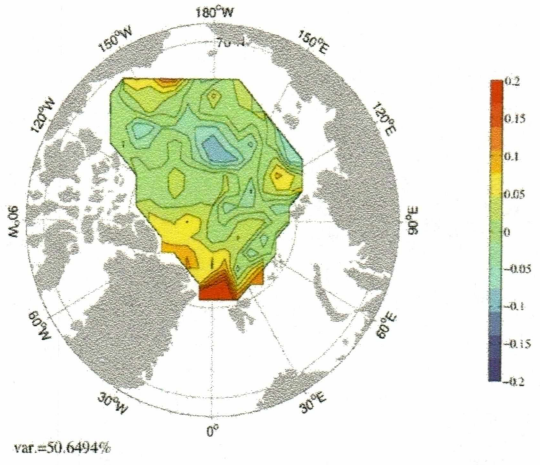

Mode 2

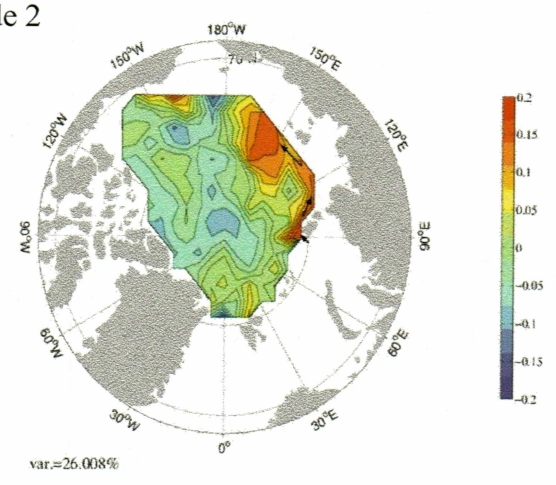

Mode 3

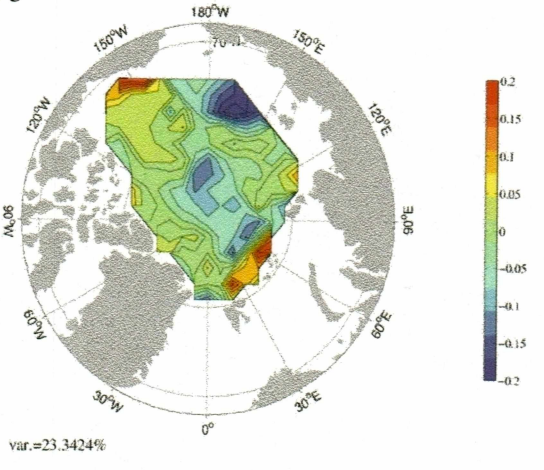

Figure 4.2 The EOFs of the central Arctic

According to Zhang et al. (1998), a strengthened Atlantic inflow both at Fram Strait and, more significantly, via the Barents Sea "flushes" out cold and fresh Arctic Water, and thus increases the temperature and salinity of the upper ocean. Therefore, when more Atlantic Water flows in through the Barents Sea, more Arctic surface water is flushed out of the Arctic Ocean and the depth to the 0°C isotherm, in the areas where the Arctic water flows out, becomes shallower.

Mode 3 shows a strong positive anomaly in the southern Beaufort Sea area and the part of the Eurasian Basin Slope between Spitsbergen and the St. Anna Trough, which might be showing the inflow of Fram Strait branch water. There is a strong negative anomaly in the part of the Siberian Shelf and the Eurasian Continental Slope in the Makarov Basin.

It is known that one should suspect contamination of modes if the variances of neighboring modes are close in value. In the analysis above, the variances of mode 2 and 3 are close to each other. According to North et al. (1982), the estimate of the *i*th EOF is most strongly contaminated by the patterns of those EOFs that correspond to the eigenvalues λ_j closest to λ_i. The smaller the difference between λ_j and λ_i, the more severe the contamination. North's rule-of-thumb is that the sampling error of a particular eigenvalue, $\Delta\lambda$, has to be comparable to or larger than the spacing between λ and a neighboring eigenvalue for the contamination:

$$\Delta\lambda_i \approx \sqrt{\frac{2}{n}}\lambda_i$$

Table 4.1 Numbers for North test (central Arctic)

Eigenvalue	Sampling error	
$\lambda_1 = 354{,}680$	$\Delta\lambda_1 = 87{,}316$	$\lambda_1 - \lambda_2 = 172{,}560$
$\lambda_2 = 182{,}120$	$\Delta\lambda_2 = 44{,}834$	$\lambda_2 - \lambda_3 = 18{,}660$
$\lambda_3 = 163{,}460$	$\Delta\lambda_3 = 40{,}241$	

The difference between λ_1 and λ_2, 172,560, is larger than the sampling errors, $\Delta\lambda_1$(87,316) and $\Delta\lambda_2$(44,834), so the modes 1 and 2 are separated. But the difference between λ_2 and λ_3, 18,660, is smaller than the sampling errors, $\Delta\lambda_2$(44,834) and $\Delta\lambda_3$(40,241). Therefore, we suspect that mode 2 and mode 3 are not separated.

Several trials were attempted to obtain the separation of modes by choosing different areas for EOF analysis. First, the EOF analysis of the Eurasian Basin and Canadian Basin were performed separately. The EOFs of the Canadian Basin were not separated, while the EOFs of the Eurasian Basin were well separated. From this it was suspected that some mechanism in the Canadian Basin acted differently for the 0°C isotherm from the one in the Eurasian Basin. The Bering Strait inflow area was noted, since the area receives Pacific-origin water, which is fresher than Atlantic Water. It was also noted that the Bering Strait inflow area in the EOFs showed the same trend in all of three modes (all positive or negative at the same time). Hence, the whole central Arctic Ocean, except for the Bering Strait inflow area, was chosen for the EOF analysis and showed the clearly separated EOFs. From these trials, we find that the EOF analysis is sensitive to change of applied area.

4.2.2 The EOF Analysis (without the Bering Strait Inflow Region)

The EOFs of the Arctic without Bering Strait inflow region (see Figure 4.3) show almost identical patterns to the ones of the whole central Arctic. The variability of each mode is 53.65%, 27.19%, and 19.16%, respectively, which is similar to the first analysis, but different enough for the separation of the modes. Table 4.2 shows the results for the North test. The difference between λ_1 and λ_2, 164,240, is larger than the sampling errors, $\Delta\lambda_1$(81,976) and $\Delta\lambda_2$(41,543), and the difference between λ_2 and λ_3, 49,840, is also larger than the sampling errors, $\Delta\lambda_2$(41,543) and $\Delta\lambda_3$(29,273). Therefore, the three modes are clearly separated, according to the North test.

From here on, the former EOFs will be used for the analysis, since the contamination is caused by relatively small Bering Strait inflow area and the two EOFs are visually similar.

Table 4.2 Numbers for North test (without the Bering Strait inflow region)

Eigenvalue	Sampling error	
$\lambda_1 = 332{,}990$	$\Delta\lambda_1 = 81{,}976$	$\lambda_1 - \lambda_2 = 164{,}240$
$\lambda_2 = 168{,}750$	$\Delta\lambda_2 = 41{,}543$	$\lambda_2 - \lambda_3 = 49{,}840$
$\lambda_3 = 118{,}910$	$\Delta\lambda_3 = 29{,}273$	

Mode 1

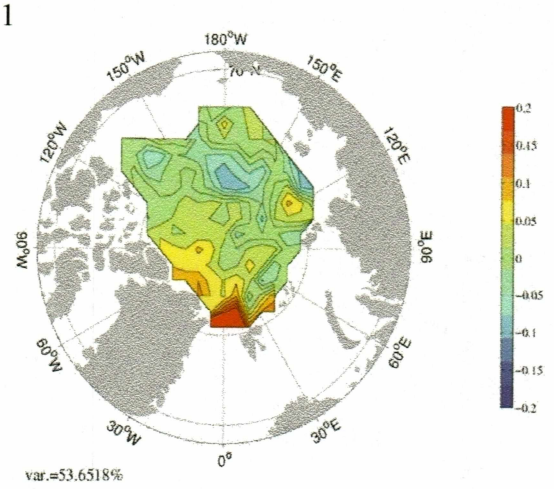

Mode 2

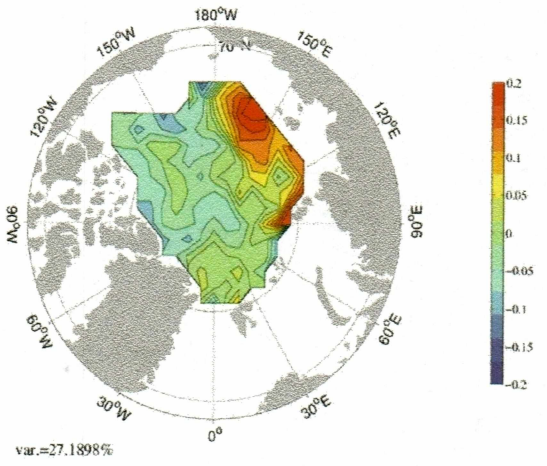

Mode 3

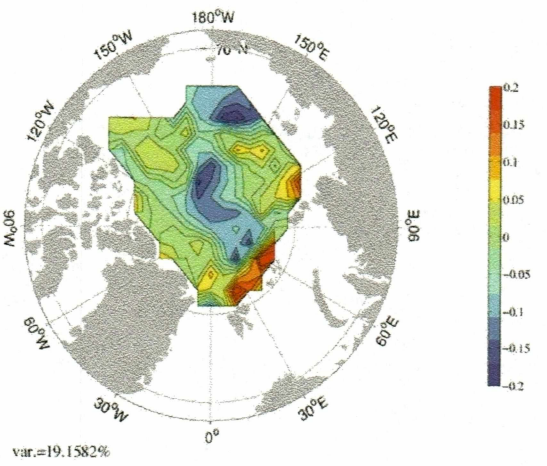

Figure 4.3 The EOFs of the Arctic (without the Bering Strait inflow region).

4.2.3 Comparison of Time Series (the Amplitude of EOFs)

Figure 4.4 shows the time series for both EOFs with and without Bering Strait shown in Figure 4.2 and 4.3. Similar to comparisons of EOFs, the time series are almost identical. The correlation coefficients for both EOFs are shown on the right side of the plot. The correlation coefficient of mode 1 is the highest, 0.99.

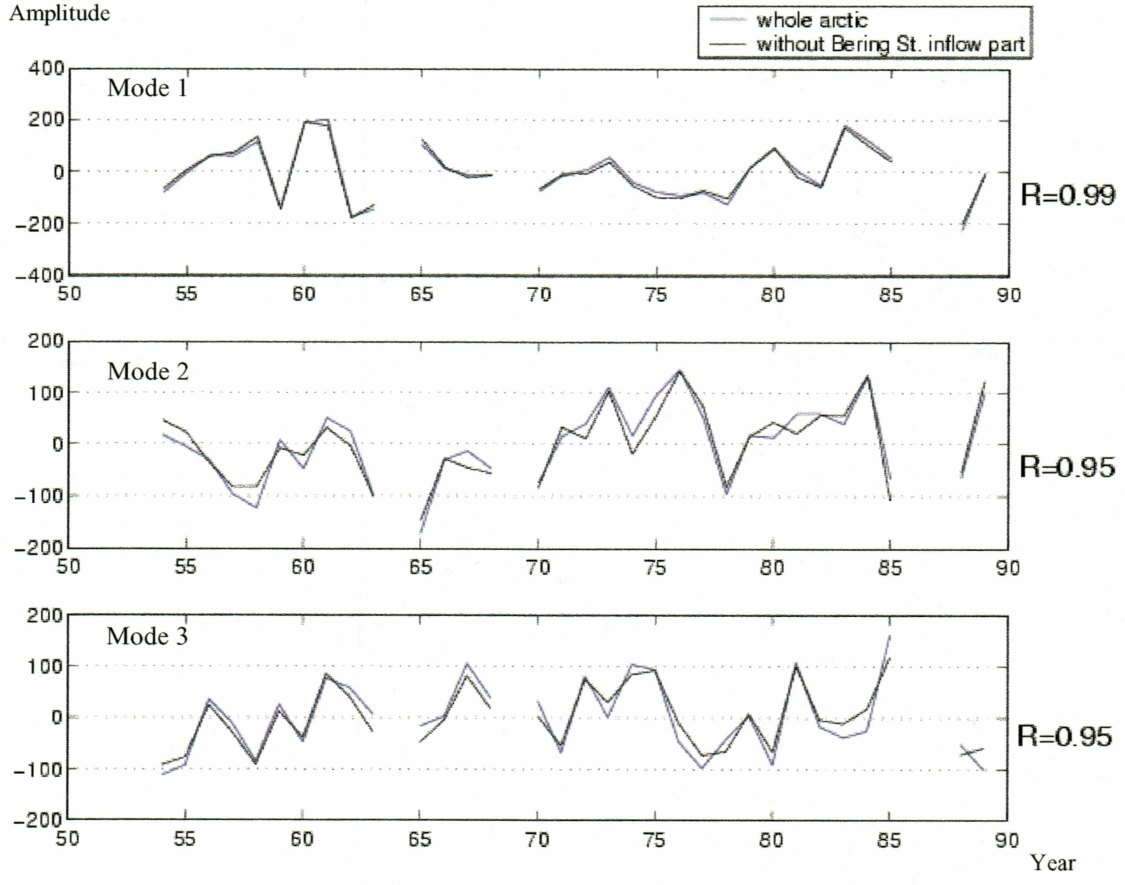

Figure 4.4 Time series of the EOF modes.

4.2.4 Correlation Maps

Figure 4.5 shows the correlation between the time series (33 points) of each point (original 0°C isotherm depth data) and the time series of the EOF modes. It is easier to see on these maps which areas are explained by which mode. In Figure 4.5.a, more than half the area of western Arctic (western side of the 0°-180° longitude) has a correlation coefficient over 0.5, while mode 1 of the EOFs shows strong variability in a much smaller area around Fram Strait. This area includes Fram Strait, an area near the Lincoln Sea, which is the major exit of the Arctic Water.

Looking at Figure 4.5.b, the area north of the Siberian Sea and the Laptev Sea, which shows high amplitude of mode 2, has correlation coefficients between 0.5-1. Although the variance of mode 2 is only 26% in the whole Arctic, this area is mostly explained by mode 2. It is more obvious in this figure that the blue color resembles the paths of the Transpolar Drift and Pacific-origin water exit to the Canadian Archipelago.

The correlation map of mode 3 (Figure 4.5.c) shows more detail than mode 3 of the EOFs. Most of the Canada Basin and the Fram Strait inflow area (the part of the Eurasian Basin Slope between Spitsbergen and St. Anna Trough) are positively correlated with mode 3.

a)

b)

c)

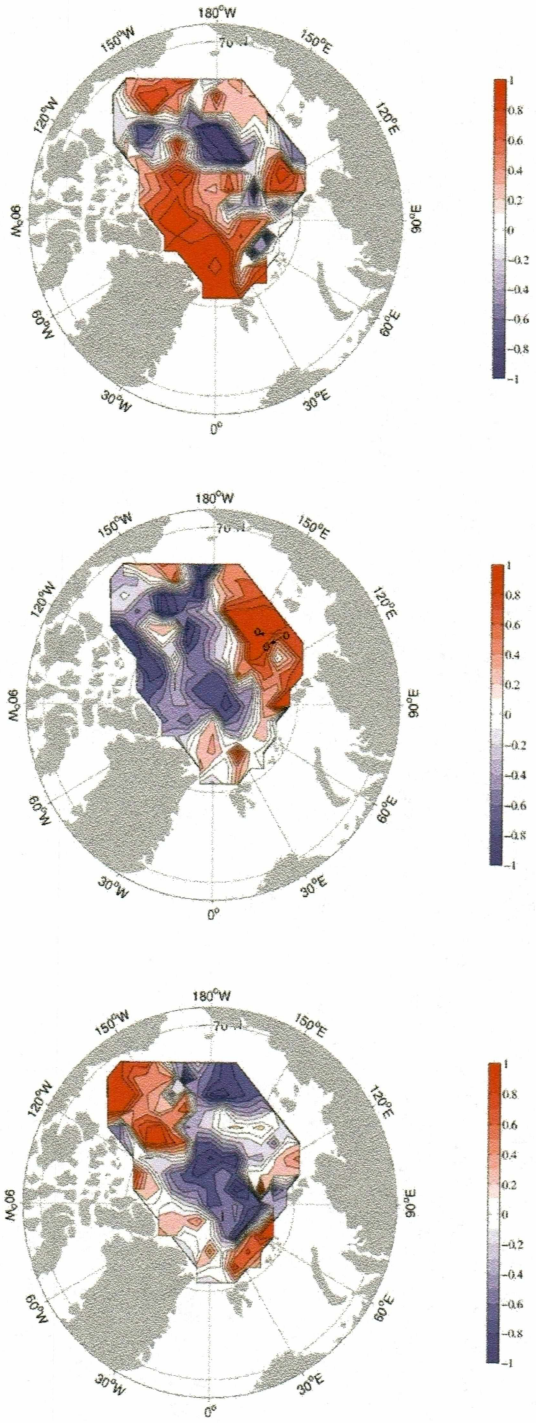

Figure 4.5 Maps showing the correlation coefficients between the time series of each point and the time series of the given EOF mode. a) mode 1; b) mode 2; c) mode 3 (points on the figure (b) shows mooring sites of Woodgate et al., 2001).

4.3 The Relationship with Atmospheric indices.

4.3.1 Atmospheric Indices

The seasonal mean (January through March) AO index is obtained from the web page of the Climate Prediction Center, National Weather Service, National Oceanic and Atmospheric Administration. The AO index is normalized using the 1950-1989 base period standard deviation. For the NAO index, the winter (December through March) index of J. Hurrell is taken from the web page of the National Center for the Atmospheric Research. The NAO index is based on the difference of normalized sea level pressure between Lisbon, Portugal and Stykkisholmur, Iceland [Hurrell, 1995]. The NAO index is also normalized using the study period standard deviation. The annual mean vorticity index is from Polyakov and Johnson (2000). The vorticity index is for the central Arctic Ocean to north of the Laptev Sea, which is computed from NCEP/NCAR sea level pressure as a finite-difference numerator of the Laplacian function [Walsh et al, 1996].

4.3.2 Comparison of the Time Series and Atmospheric Indices

The time series of the first three modes were compared with the atmospheric indices for both correlation and lagged correlation (crosscorrelation). For a proper comparison, the time series were also normalized, dividing by the standard deviation. Mode 2 and the AO index have the highest correlation (0.58) of all the indices and the three modes. Mode 2 and the NAO index have the second highest correlation coefficient, 0.57. Both are significantly correlated at the 99% level. Mode 2, having

high correlation with both the AO and NAO index, is probably because of the close correlation of both indices [Deser, 2000]. However, the NAO and mode 2 have a significant 1 year lagged correlation, which is led by the NAO (correlation coefficient, 0.48, 99% level), while the AO does not have any lagged correlation with mode 2.

The vorticity index shows a significant correlation with mode 3 (correlation coefficient, 0.45), when the vorticity index leads by 1 year. The vorticity index also has a high correlation with mode 1 (correlation coefficient, 0.49), when mode 1 leads by 3 years. Figure 4.6 shows the related modes and indices together.

The significant relationship of mode 2 and the AO index (or NAO index) suggests that the depth to the 0°C isotherm is affected by the atmosphere, especially in the area where the water from the Barents Sea flows into the Arctic Ocean, connecting to the Eurasian Basin Slope and to the Makarov Basin Slope. If a situation is assumed for high AO index (or NAO), which characterizes a weakening of the Beaufort high pressure cell and a strengthening of the Iceland low pressure cell, there is more Atlantic Water flowing into the Arctic through both Fram Strait and the Barents Sea, especially more through the Barents Sea [Loeng et al., 1997; Zhang et al., 1998]. Since mode 2 describes the variability of the Barents Sea inflow into the Arctic Ocean, it can be interpreted that more than the average amount of Barents Sea water flows into the Arctic above the 0°C isotherm and mixes with the Fram Strait branch water, and that the mixing with colder inflow deepens the depth to the 0°C isotherm in years of high AO index. The 0°C depth in the path of the

Transpolar Drift and the exit flow area through the Canadian Archipelago become shallower in the high AO index years.

A model study by Karcher and Oberhuber (2002) showed that the inflow from the Barents Sea into the Arctic Ocean covers a variety of densities. They showed that the lightest water from the shelf joins the polar surface mixed water, feeds the Siberian branch of the Transpolar Drift, and reaches Fram Strait after 3-6 years. They also argued that the medium density water from the Barents Sea, which is lighter than the Fram Strait branch Atlantic Water, feeds the halocline. These results of Karcher and Oberhuber suggest that a stronger inflow from the Barents Sea induces a stronger outflow through Transpolar Drift. Their results also support the idea that the colder but lighter water from the Barents Sea joins the Fram Strait branch Atlantic Water, resulting in deepening of the 0°C isotherm.

Since the AO index can change from positive to negative daily and/or monthly, a couple months of high AO index may induce an increased inflow from the Barents Sea. Woodgate et al. (2001) showed a sudden decrease in temperature and salinity of the Atlantic layer core at moorings (deployed along three slope sites spanning the junction of the Lomonosov Ridge with the Eurasian Continent). Their data also showed the propagation of this change (one passing over the Lomonosov Ridge from the Eurasian Basin and the other following the counterclockwise turn in the Eurasian Basin, Figure 4.5 (b)) in their year-long mooring time series (1995-1996). They concluded that the cooling and freshening was due to a change in the quantity and/or properties of the Barents Sea branch waters intruding and mixing with the Fram

Strait branch water. The result above supports the idea that the change in the inflow from the Barents Sea to the Arctic is often caused by a change in the atmospheric conditions.

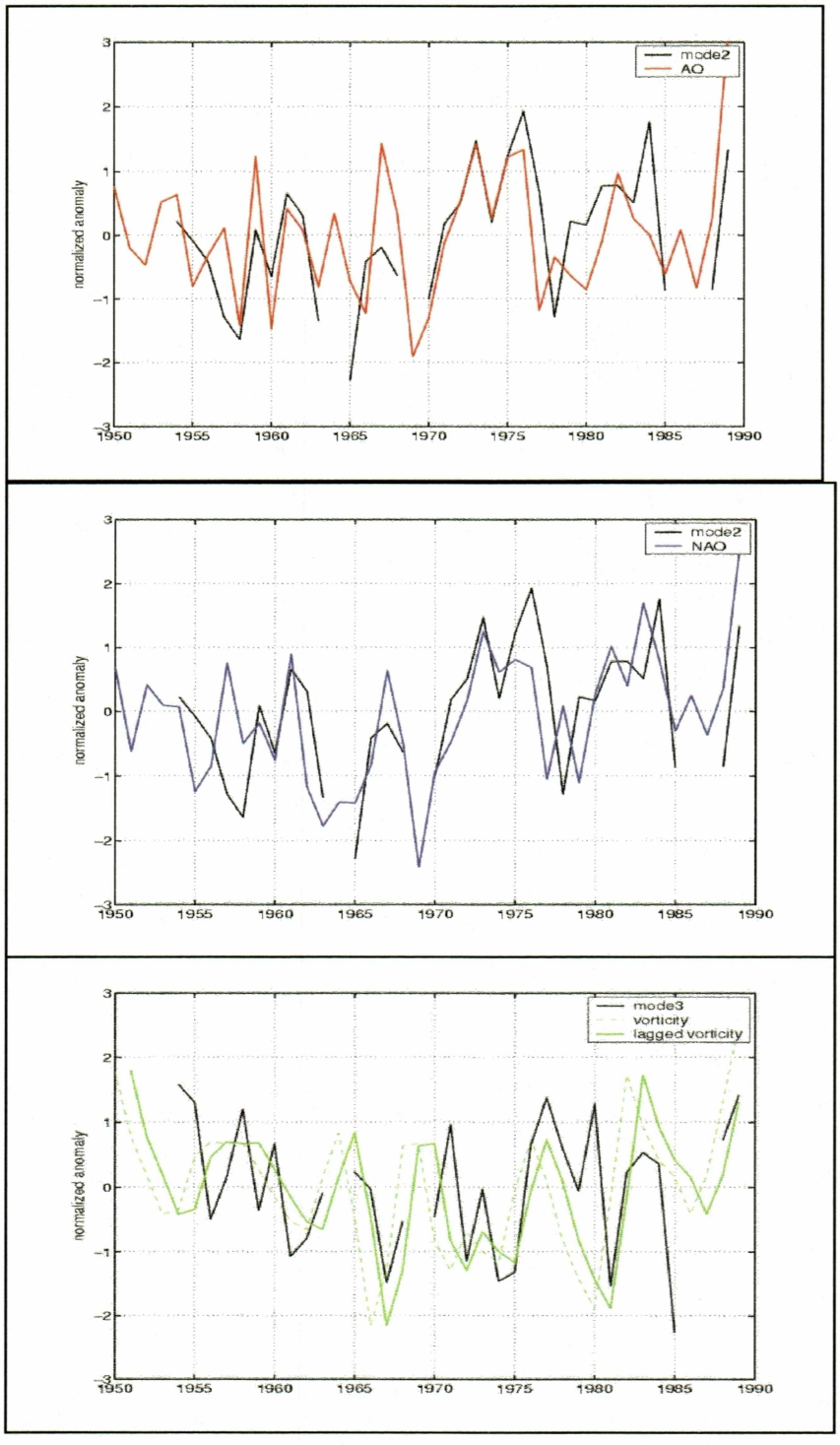

Figure 4.6 Comparison of atmospheric indices and EOF time series. AO index and mode 2 time series (Top), NAO index and mode 2 time series (Middle), The vorticity index and mode 3 time series (Bottom); the sign of mode 3 time series is changed for ease of comparison.

4.3.3 Composites Using Atmospheric Indices

To gain a better physical understanding of the 0°C depth pattern, composite maps are produced based on the AO index, NAO index, and Arctic annual mean vorticity index (here after vorticity index). The data are divided into high index years and low index years, which are shown in table 4.3. The composite maps are formed from the difference between the high and low years. Figure 4.7.a shows the composite maps. AO and NAO composite maps have a pattern similar to the spatial map of mode 2, which is consistent with the AO and NAO indices having high correlation coefficients with the time series of mode 2. For the vorticity composite map, there is an inversely similar pattern to the spatial map of mode 3, which has a strong negative anomaly in the Beaufort Sea and the part of the Eurasian Basin Slope between Spitsbergen and the St.Anna Trough and a strong positive anomaly in the part of the Siberian Shelf and the Eurasian Continental Slope in the Makarov Basin.

Table 4.3 High atmospheric indices years and low atmospheric indices years

	High Indices Years	Low Indices Years
AO	50,54,57,59,61,62,67,68,72,73, 74,75,76,82,83,84,88,89	55,56,58,60,63,65,66,70,71,77,78, 79,80,81,85
NAO	50,54,57,61,67,72,73,74,75,76, 78,80,81,82,83,84,88,89	55,56,58,59,60,62,63,65,66,68,70, 71,77,79,85
Vorticity	50,55,56,57,58,59,63,68,76,77, 82,83,84,85,88,89	54,60,61,62,65,66,67,70,71,72,73, 74,75,78,79,80,81

Figure 4.7.b shows the correlation map between the original 0°C depth time series and each of the atmospheric indices. The correlation maps show that the data are correlated with the atmospheric indices in the same pattern as EOFs and composites. Both a composite map and a correlation map show similar patterns for each index. The vorticity correlation map is made with 1 year lagged vorticity index and the data of each point, since 1 year lagged vorticity is negatively correlated with mode 3.

These maps are drawn without any information from the EOF study. This suggests that the EOF modes in this study are not just showing mathematical partitions but showing that the EOF patterns are related to physical forcing.

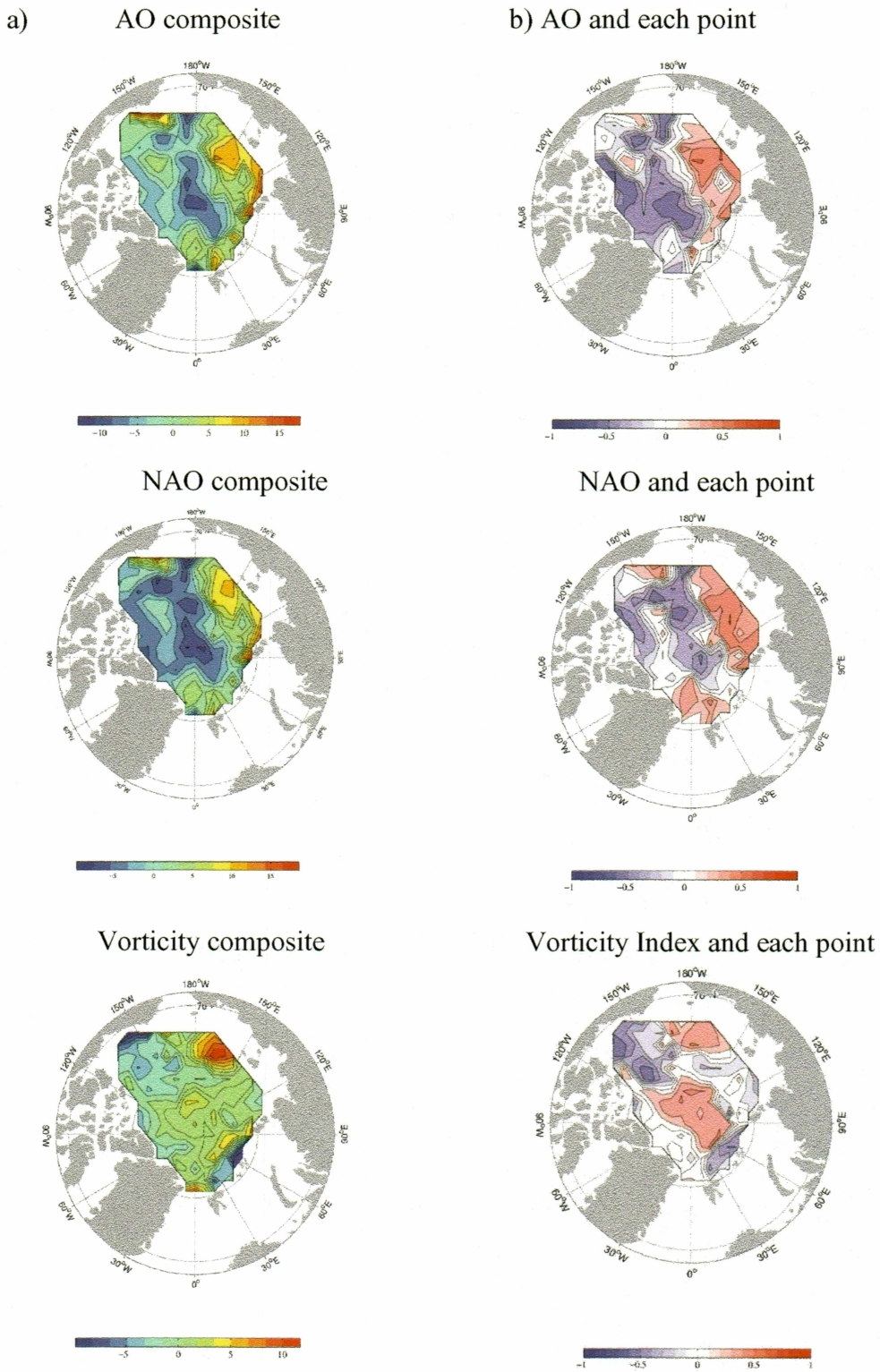

Figure 4.7 (a) Composite maps (the difference of data between high indices years and low indices years in meters) and (b) correlation coefficient maps.

4.4 Section Maps of 0°C Isotherm Depth Anomaly

Maps of the anomaly of the depth to the 0°C isotherm versus time are shown in Figure 4.9 to show variability of the original data at selected locations with high variability. Missing data years are not labeled, but the data for those years were linearly interpolated. Six selected locations are shown in Figure 4.8. Section (a) is an area where the Barents Sea water flows into the Arctic Ocean, section (b) shows the Atlantic Water after passing the Lomonosov Ridge, and section (c) is near Sverdrup Islands. Sections (a), (b), and (c) have high variability with section (c) having opposite sign of sections (a) and (b) in mode 2. Section (d), Fram Strait is chosen for the overall highest variability. Section (e), which is close to the Alaskan coast, is chosen for its proximity to the Bering Strait inflow. Section (f) is near the Lincoln Sea and was selected because this area is where the Arctic Water exits to Baffin Bay and because this region has high variability for mode 1. Both sections (c) and (f) are adjacent to the Canadian Archipelago, but (c) has higher amplitude in mode 2 and (f) has higher amplitude in mode 1. The x axis shows the data point (2-4 data points for each section) and the anomaly values are in meters.

Looking at Figure 4.9.A, sections (a) and (b) have very similar variability and section (c) has smaller amplitudes with generally opposite signs of the other two sections. Sections (a) and (b) have a noticeable negative anomaly in the years of 1957-1958, 1963-1965, and 1984, and a strong positive anomaly in 1973, 1975-1977, 1984, and 1989. Section (c) has the same anomaly but opposite sign as section (a) and (b) at most times, except for a positive anomaly in 1960-1961. These results

suggests that a deepening of the 0°C isotherm where the Barents Sea water flows into the Arctic Ocean, concurs with a shallowing of the 0°C isotherm where the Arctic Surface Water exits through the Canadian Archipelago.

For Figure 4.9.B, sections (d) and (f) have some strong positive/negative anomalies at the same time. These two sections are locations where the Arctic Water exits to Fram Strait and Baffin Bay and there is high variability of mode 1. Section (e) can be divided in two smaller sections, since section (e) points 1-2 shows some different variability from that of the section (e) points 3-4 (sometimes points 1-3 and 4). Pacific-origin water is known to flow through section (e) and exits the Arctic Ocean through the Canadian Archipelago or Fram Strait [Mclaughlin et al., 2002]. Section (c) and (f) are both Pacific-origin water passages of the Canadian Archipelago, but section (c) and (f) have different variability in the EOFs of this study. Some examples of different variability can be found in the anomaly section maps. A strong positive signal occurred in 1983-1984 for section (e) 3-4 but in 1984-1985 for section (e) 1-2. This 1983-1984 signal in section (e) 3-4 had its concurrent match only in section (f), not in section (c). In section (e) 1-2, there was a noticeable positive signal in 1967. Both sections (c) and (f) had a similar signal at this time. These two different types of variability in section (e) might reflect the two different pathways of Pacific Water inflow.

This section of the chapter shows in another way that the anomaly of 0°C isotherm depth is regionally variable and agrees with the results of the EOFs and time series of the analysis.

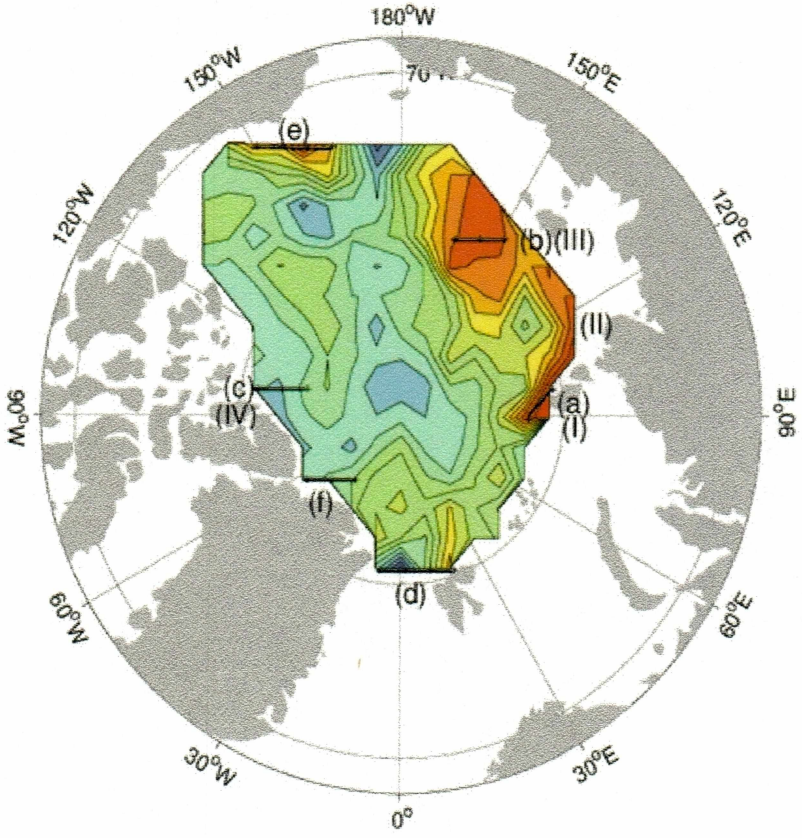

Figure 4.8 Locations for section maps (a, b, c, d, e, f) and temperature profiles (I, II, III, IV). (a) section where the Barents Sea Water flows out, (b) section north of Ostrova Islands, (c) section near Svedrup Islands, (d) Fram Strait section, (e) section close to Alaskan coast, (f) section near the Lincoln Sea, (I): the Barents Sea outlet area; (II): an area neighboring the Laptev Sea; (III): an area neighboring the Siberian Sea; (IV): an area neighboring Svedrup Islands). Locations are shown over the second EOFs.

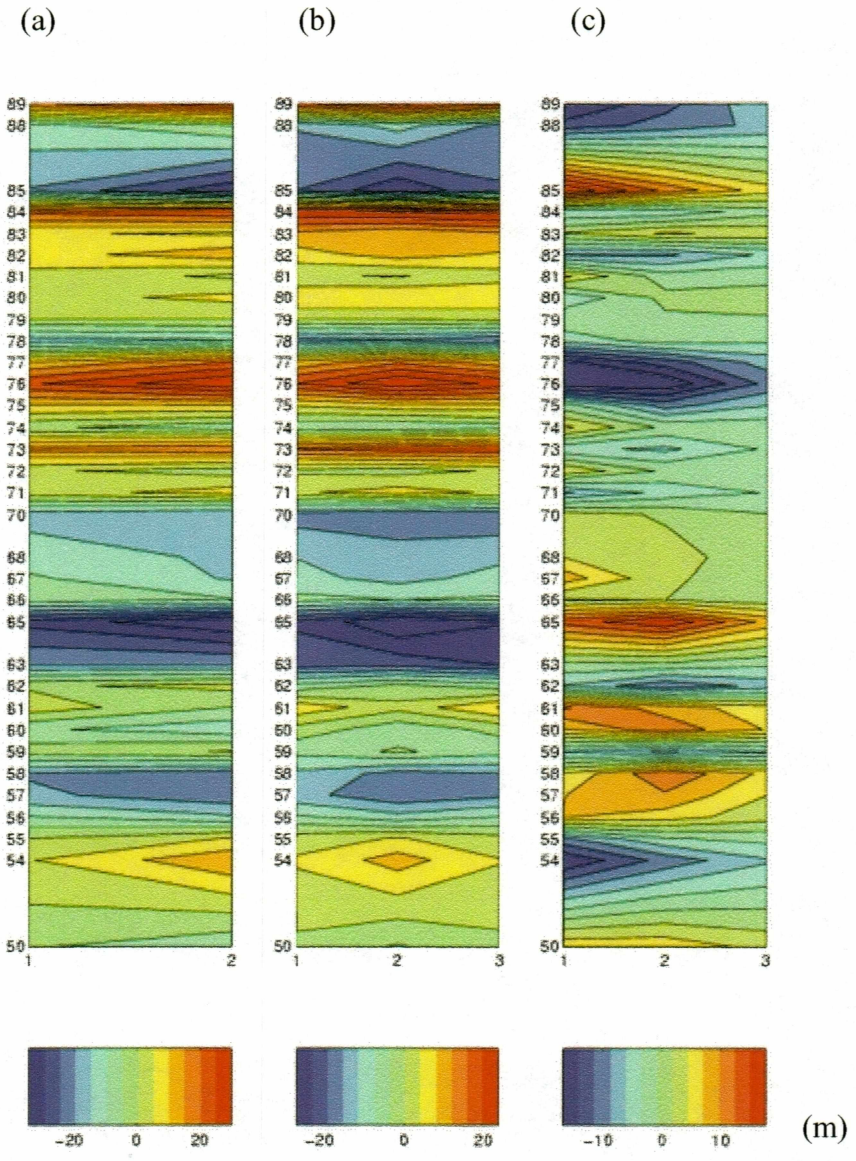

Figure 4.9.A) Section maps of anomaly of depth to the 0°C isotherm.

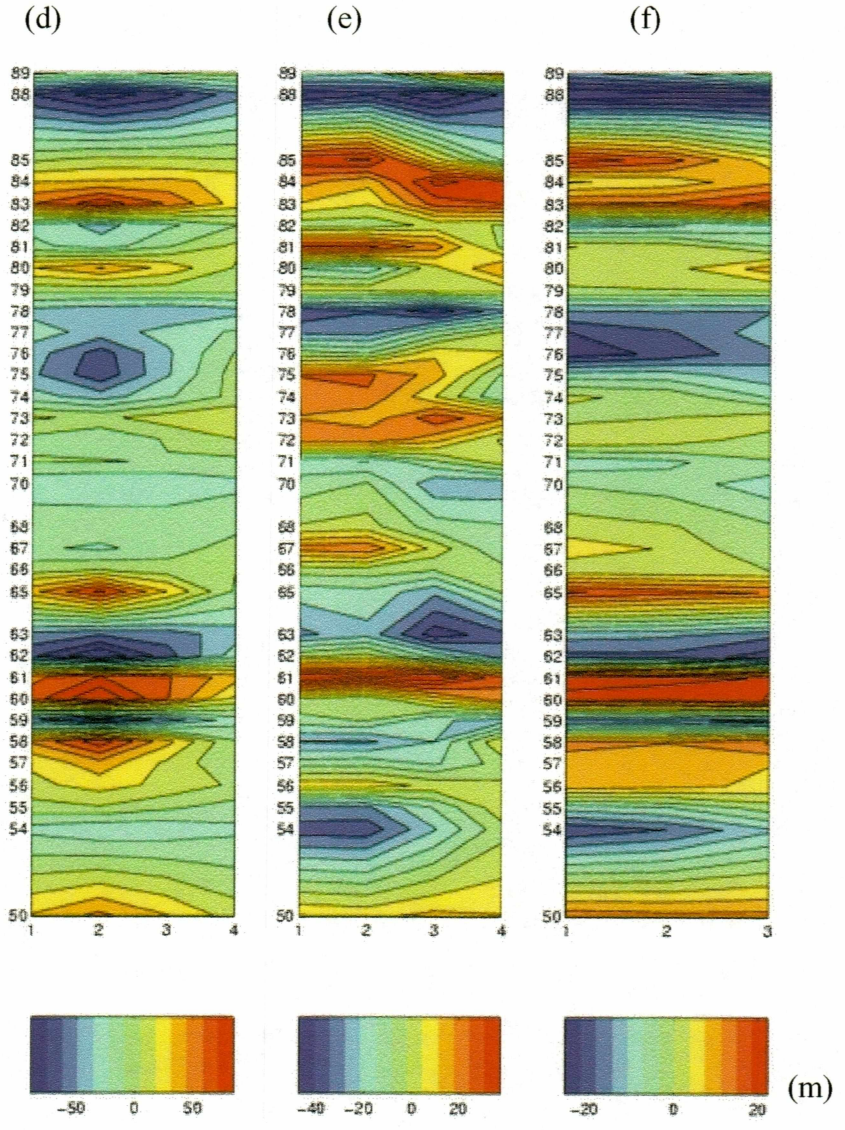

Figure 4.9.B) Section maps of anomaly of depth to the 0°C isotherm.

4.5 Temperature Profiles at Selected Locations

Vertical temperature profiles of EWG hydrographic data were examined to see if there is variability in the thickness of Atlantic water (>0°C water), and to see if the thickness of Atlantic Water and the 0°C depth are related. The grid of temperature data is different from that of the 0°C depths data. The area covered is also slightly different along the edges from the 0°C depth data. Four selected locations are shown in Figure 4.8. Location (I) is the Barents Sea water outlet area, location (II) is an area neighboring the Laptev Sea, location (III) is an area neighboring the Siberian Sea, and location (IV) is an area neighboring the Sverdrup Islands. Profiles are displayed in order following the counterclockwise Atlantic Water flow in Figure 4.10. These locations were chosen for higher variability in mode 2. (I), (II), and (III) have the same sign and (IV) has the opposite sign in mode 2.

Since the data are only given in decadal averages, there are four profiles at any point for the 40 year period. Locations (I) and (II), which have more impact from the Barents Sea input, show more decadal variability than locations (III) and (IV). Location (I) has temperature profiles with two local maxima. Considering that the shallower part of the Barents Sea water is colder than the Fram Strait branch water, the shallower peak can be interpreted as the water mixed with colder water coming out of the Barents Sea, and the deeper peak is warmer Fram Strait branch water. By the time these waters arrive in location (II), the temperature profiles show only one maximum, indicating that the two water masses have mixed.

Location (I) shows the most variability in the thickness of Atlantic Water in the chosen areas. Location (II) has much less variability and locations (III) and (IV) show little variability. In location (I) profiles, it is hard to find the relationship between the depths to the 0°C isotherm and the thickness of Atlantic Water. Considering two branches of Atlantic Water flowing through Fram Strait and the Barents Sea with different volumes at different times, it will not be easy to find any trend, particularly from decadal data.

The results from this section of the chapter suggest that the depth to the 0°C isotherm becomes deeper with more inflow of Barents Sea branch water.

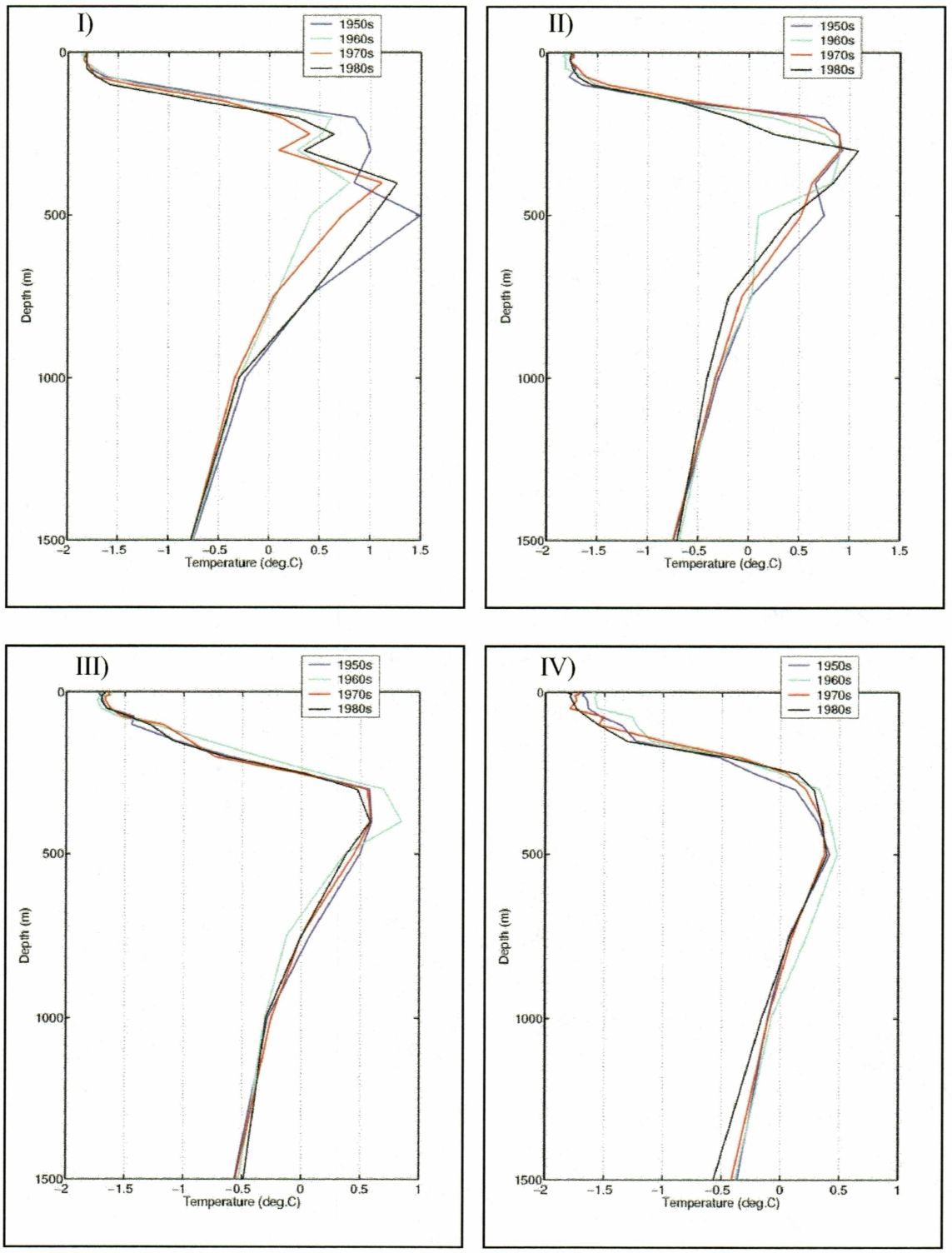

Figure 4.10 Temperature profiles at selected locations.

Chapter 5. Summary and Discussion

EOF analyses were performed on data describing the depth to the 0°C isotherm field in the Arctic Ocean. The time series of the EOFs were compared with several atmospheric indices. The second mode of the EOFs was significantly correlated with the AO index (correlation coefficient, 0.58). The third mode was significantly correlated with the vorticity index (correlation coefficient, 0.45) when the vorticity index leads by 1 year. The second mode showed the variability in inflow from the Barents Sea and the variability in outflow from the Arctic Ocean, possibly induced by the change of the Barents Sea inflow through continuity. An increase in the inflow of the Barents Sea water causes a deepening of the 0°C isotherm because an increase of the Barents Sea water occurs stronger in the surface layer, which is above the 0°C isotherm. Deepening occurs also because the upper Barents Sea water is colder than Fram Strait branch water. A stronger increase in the inflow of the upper Barents Sea water flushes out the surface water, which causes the depth to the 0°C isotherm to shoal in the region where the surface water flows out.

Composite analyses of the data using the atmospheric indices (AO, NAO, and vorticity index) were performed. A composite map of the data using the AO (or NAO) index showed a pattern similar to the second EOF. This validates a high correlation between the time series of mode 2 and the AO (or NAO) index. Section maps of the 0°C isotherm depth anomaly in time also verify that the EOF analysis of

this study is valid. The sections with high variability in mode 2 have the same high or low anomalies as the time series of mode 2.

The path of Fram Strait branch water is not obvious from the EOFs, while the second EOF shows the change of inflow of the upper Barents Sea water with its path in the Arctic Ocean. Mode 1 has high amplitudes in the area between Spitsbergen and Franz Josef Land. Mode 3 also shows high amplitudes in the section between the area north of Spitsbergen and the St. Anna Trough. Both are probably related to inflow of Fram Strait branch Atlantic Water. Since the depth to the 0°C isotherm is around 100m in the southern Eurasian Basin, the change of Barents Sea inflow has a stronger effect on the 0°C isotherm than the change in Fram Strait branch water. It is suggested that the path of Fram Strait branch water is less obvious in the 0°C isotherm analysis due to its deeper depth. This agrees with Zhang et al. (1998), who claimed that Barents Sea branch water is more sensitive to atmospheric pressure and wind patterns than Fram Strait branch water, probably due to the shallow bathymetry of the Barents Sea.

Previous work showed that the Barents Sea branch Atlantic Water inflow into the Arctic Ocean occurs between Novaya Zemlya and Franz Josef Land into the Kara Sea then down through the St. Anna Trough [Rudels et al., 1994; Rudels and Friedrich, 2000; Schauer et al., 2002]. However, the second EOF of this study shows that the change of the Barents Sea inflow occurs closer to the Voronin Trough, which is roughly 180km east of the St. Anna Trough. It means that the shallower part (the surface water) of the Barents Sea Water flows out more through the Voronin Trough

than the St. Anna Trough. According to yearly mean velocities from four mooring measurements between Novaya Zemlya and Franz Josef Land by Schauer et al. (2002), one mooring shows strong velocities towards the St. Anna Trough, and the other three are flowing eastward (passing by the St. Anna Trough) with weaker velocities. This suggests that the Kara Sea is receiving much of the Barents Sea water and this water does not all exit through the St. Anna Trough, leaving the possibility of strong inflow through the Voronin Trough. There are at least two reasons why the second EOF shows stronger inflow through the Voronin Trough. 1) The Voronin Trough is shallower than the St. Anna Trough, hence the change through the Voronin Trough has more impact on the 0°C isotherm than that of the St. Anna Trough. 2) Perhaps more of the Barents Sea Water flows through the Voronin Trough than the St. Anna Trough at shallower depths (shallower than the 0°C isotherm), when there is a higher inflow through the Barents Sea, which mostly happens during the winter season. Karcher and Oberhuber (2002) also showed that the Barents Sea branch water flows through the Voronin Trough, while the Fram Strait branch water flows through the St. Anna Trough.

McLaughlin et al. (2002) hypothesized that there are two Arctic atmosphere-ocean modes, explaining Arctic Ocean circulation and freshwater export with two different atmospheric systems (building on the anticyclonic and cyclonic systems of Proshutinsky and Johnson, 1997). McLaughlin et al. argued that the increase of Atlantic inflow, especially through the Barents Sea during cyclonic atmospheric system, displaces the Pacific-origin fresh water mainly through the Canadian

Archipelago, which is consistent with the result of this study. According to the patterns of mode 2 (figure 4.2 & 4.5), the increase of the Barents Sea branch water during a high AO (NAO) index coincides with the exit through the Canadian Archipelago except for the Lincoln Sea. The variability around the Lincoln Sea is explained by mode 1, not mode 2, which means that the variability around the Lincoln Sea is similar to that of Fram Strait, not with other Canadian Archipelago exits. This suggests that there could be different processes in the exit flow of the Arctic Water through the Lincoln Sea

What drives changes in the depth to the 0°C isotherm in the Arctic Ocean? The 0°C isotherm is determined by changes in two water masses, the Surface water and the Atlantic layer. In this study, the atmospheric condition is one of the major factors in the variation of the depth to the 0°C isotherm. The atmosphere over the Arctic Ocean affects the surface layer and below. The atmosphere over the GIN Sea and/or the North Atlantic Ocean affects the Atlantic water inflow (temperature and strength) into the Arctic, especially through the Barents Sea, and hence has an influence on the 0°C isotherm in the Arctic Ocean. This study showed that the annual mean vorticity index, which can represent the atmosphere over the Arctic Ocean, is significantly correlated with mode 3. A significant correlation between the time series of mode 2 and the AO (NAO) index verifies that there is a strong relationship between the atmosphere over the GIN Sea and the North Atlantic Ocean and the 0°C isotherm of the Arctic Ocean. From the results of this study, not only the atmosphere over the Arctic Ocean, but also the atmosphere over the GIN Sea and North Atlantic Ocean

affects the 0°C isotherm in the Arctic Ocean. The results of this study also suggest that the Atlantic inflow through the Barents Sea affects the surface currents of the Arctic Ocean, changing the strength of Transpolar Drift and the exit flow through the Canadian Archipelago.

Chapter 6. Conclusion

EOF analyses of the depth to the 0°C isotherm of the Arctic Ocean were performed. The data are from the "Environmental Working Group – Joint U.S. Russian Atlas of the Arctic Ocean". The conclusions of this study are as follows:

The EOF analysis of the depth to the 0°C isotherm in the Arctic Ocean explained 99% of the variability with the first three modes. The variances of the first three modes were 51%, 26%, and 23%, respectively.

Mode 1 mainly showed the variability of the outflow through Fram Strait and the Lincoln Sea. The Lincoln Sea showed different variability from the other exit passages of the Arctic water into the Canadian Archipelago, which are considered as exits of Pacific-origin fresh water. The Lincoln Sea was highly correlated with the first mode, while other passages to the Canadian Archipelago were correlated with the second mode.

Mode 2 showed the variability of the inflow of the Barents Sea branch Atlantic water and the variability of the outflow through the Canadian Archipelago and Trans polar Drift, which were induced by the inflow through the Barents Sea. The variability of the inflow of the Barents Sea branch water has a close correlation with atmospheric conditions (AO or NAO index). The second mode of the EOF analysis supported that

the Barents Sea water flows out more through the Voronin Trough than through the St. Anna Trough at shallower depths, when there is a higher inflow through the Barents Sea.

Mode 3 was significantly correlated with the annual mean vorticity index, when the vorticity index leads by 1 year. Mode 3 showed high amplitudes in the section between the area north of Spitsbergen and the St. Anna Trough, which was probably related with the inflow of the Fram Strait branch Atlantic Water.

Composite analyses of the data using AO, NAO, and Arctic vorticity indices confirmed that the EOF analysis results of this study can be related to atmospheric driving. A composite map using the AO (NAO) index showed a pattern similar to the second EOF. Hence, it supported that the AO index and the second mode are correlated. A composite map using the vorticity index had a pattern similar to the third EOF.

This study showed that the 0°C isotherm in the Arctic Ocean contains much information that might allow us to further understand the characteristics of the Arctic Ocean.

References

Aagaard, K., P. Greisman, 1975, Towards new mass and heat budgets for the Arctic Ocean, J. Geophys. Res., 80, 3821-3827.

Aagaard, K., 1981, On the deep circulation of the Arctic Ocean, Deep-Sea Res., 28, 251-268.

Aagaard, K., L. K. Coachman, and E. C. Carmack, 1981, On the halocline of the Arctic Ocean, Deep-Sea Res., 28, 529-545.

Aagaard, K., J. H. Swift, and E. C. Carmack, 1985, Themohaline Circulation in the Arctic Mediterranean Seas, J. Geophys. Res., 90, 4833-4846.

Aagaard, K., A. Foldvik, and S. R. Hillman, 1987, The West Spitsbergen Current: Disposition and Water Mass Transformation, J. Geophys. Res., 92, 3778-3784.

Aagaard, K., and E. C. Carmack, 1989, The Role of Sea Ice and Other Fresh Water in the Arctic Circulation, J. Geophys. Res., 94, 14485-14498.

Aagaard, K., 1989, A synthesis of the Arctic Ocean Circulation, Rapp. P.-v. Réun. Cons. int. Explor. Mer., 188: 11-22.

Ådlandsvik, B., and H. Loeng, 1991, A study of the climatic system in the Barents Sea, Polar Res., 10, 45-49.

Anderson, L. G., G. Bjørk, O. Holby, E. P. Jones, G. Kattner, K. P. Kolter-Mann, R. Liljeblad, R. Lindgren, B. Rudels, and J. Swift, 1994, Water masses and circulation in the Eurasian Basin: Results from the Oden 91 expedition, J. Geophys. Res., 99, 3273-3283.

Blindheim, J., V. Borovkov, B. Hansen, S.-Aa. Malmberg, W. R. Turrel, and S. Østerhus, 2000, Upper layer cooling and freshening in the Norwegian Sea in relation to atmospheric forcing, Deep Sea Res. I, 47, 655-680.

Bourke, R. H., A. M. Weigel, and R.G. Paquette, 1988, The Westward Turning Branch of the West Spitsbergen Current, J. Geophys. Res., 93, 14065-14077.

Carmack, E.C., 1990, Large-Scale Physical Oceanography of Polar Oceans, in W.O. Smith Jr.(ed.) Polar Oceanography, Part A, Academic Press, San Diego, California, 171-212.

Deser, C., 2000, On the Teleconnectivity of the "Arctic Oscillation", Geophys. Res. Lett., 27, 6, 779-782.

Dickson, R. R., T. J. Osborn, J. W. Hurrell, J. Meincke, J. Blindheim, B. Adlandsvik, T. Vinje, G. Alekseev, and W. Maslowski, 2000, The Arctic Ocean Response to the North Atlantic Oscillation, J. Climate, 13, 2671-2696.

Emery, W. J. and R.E. Thomson, 2001, Data Analysis Methods in Physical Oceanography, Second and Revised Edition, 638pp.

Fahrbach, E., J. Meincke, S. Østerhus, G. Rohardt, U. Schauer, V. Tverberg, and J. Verduin, 2001, Direct measurements of volume transports through Fram Strait, Polar Res., 20, 217-224.

Grotefendt, K, K. Logemann, D. Quadfasel, and S. Ronski, 1998, Is the Arctic Ocean warming?, J. Geophys. Res., 103, 27679-27687.

Hurrell, J.W., 1995, Decadal trends in the North Atlantic Oscillation: Regional temperatures and precipitation, Science, 269, 676-679.

Jones, E.P., 2001, Circulation in the Arctic Ocean, Polar Res., 20, 139-146.

Karcher, M. J., and J. M. Oberhuber, 2002, Pathways and modification of the upper and intermediate waters of the Arctic Ocean, J. Geophys. Res., 107(C6), 10.1029/2000JC000530.

Loeng, H., V. Ozhigin, and B. Ådlandsvik, 1997, Water fluxes through the Barents Sea, J. Marine Science, 54, 310-317.

McLaughlin, F., E. Carmack, R. Macdonald, A. J. Weaver, and J. Smith, 2002, The Canada Basin, 1989-1995: Upstream events and far-field effects of the Barents Sea, J. Geophys. Res., 107, C7, 10.1029/2001JC000904.

Morison, J., M. Steele, and R. Andersen, 1998, Hydrography of the upper Arctic Ocean measured from the nuclear submarine USS Pargo, Deep Sea Res. I, 45, 15-38.

Morison, J., K. Aagaard, and M. Steele, 2000, Recent Environmental Changes in the Arctic: A Review, Arctic, 53, 4, 359-371.

North, G. R., T. L. Bell, R. F. Cahalan, and F. J. Moeng, 1982, Sampling Errors in the Estimation of Empirical Orthogonal Functions, Mon. Wea. Rev., 110, 699-706.

Polyakov, I. V., and M. A. Johnson, 2000, Arctic decadal and interdecadal variability, Geophys. Res. Lett., 27, 4097-4100.

Proshutinsky, A. Y., and M. A. Johnson, 1997, Two circulation regimes of the wind-driven Arctic Ocean, J. Geophys. Res., 102, 12,493-12,514.

Proshutinsky, A. Y., I. V. Polyakov, and M. A. Johnson, 1999, Climate states and variability of Arctic ice and water dynamics during 1946-1997, Polar Res., 18, 135-142.

Rudels, B., A-M. Larsson and P-I. Sehlstedt, 1991, Stratification and water mass formation in the Arctic Ocean: some implications for the nutrient distribution, Proceedings of the Pro Marc Symposium on Polar Marine Ecology, 19-31.

Rudels, B., E. P. Jones, L. G. Anderson, and G. Kattner, 1994, On the Intermediate Depth Waters of the Arctic Ocean, in The Polar Oceans and Their Role in Shaping the Global Environment, Johannessen et al.(ed.), 33-46.

Rudels, B. and Friedrich, H.J., 2000, The transformations of Atlantic Water in the Arctic Ocean and their significance of the freshwater budget, in The Freshwater Budget of the Arctic Ocean, E.L. Lewis et al.(ed.), 503-532.

Schauer, U., H. Loeng, B. Rudels, V. K. Ozhigin, and W. Dieck, 2002, Atlantic Water flow through the Barents and Kara Seas, Deep Sea Res. I, 49, 2281-2298.

Smethie Jr., W. M., P. Schlosser, G. Bönisch, and T. S. Hopkins, 2000, Renewal and circulation of intermediate waters in the Canadian Basin observed on the SCICEX 96 cruise, J. Gephys. Res., 105, 1105-1121.

Steele, M., and T. Boyd, 1998, Retreat of the cold halocline layer in the Arctic Ocean, J. Gephys. Res., 103, 10419-10435.

Swift, J. H., E. P. Jones, K. Aagaard, , E. C. Carmack, M. Hingston, R. W. Macdonald, F.A. McLaughlin, and R. G. Perkin, 1997, Waters of the Makarov and Canada basins, Deep Sea Res., 44, 1503-1529.

Thompson, D.W., and J. M. Wallace, 1998, The Arctic Oscillation signature in the wintertime geopotential height and temperature fields, Geophys. Res. Lett., 25, 9, 1297-1300.

Tomczak, M., and J. S. Godfrey, 1994, Regional Oceanography: An Introduction, Pergamon, 422 pp.

Walsh, J. E., W. L. Chapman, and T. L. Shy, 1996, Notes and Correspondence: Recent Decrease of Sea Level Pressure in the Central Arctic, J. Climate, 9, 480-486.

Woodgate, R.A., K. Aagaard, R.D. Muench, J. Gunn, G. Björk, B. Rudels, A.T. Roach, and U. Schauer, 2001, The Arctic Ocean Boundary Current along the Eurasian slope and the adjacent Lomonosov Ridge: Water mass properties, transports and transformations from moored instruments, Deep Sea Res. I, 48, 1757-1792.

Zhang, J., D. A. Rothrock, and M. Steele, 1998, Warming of the Arctic Ocean by a strengthened Atlantic inflow: Model results, Geophys. Res. Lett., 25, 1745-1748.